PERGAMON

Journal of Structural Geology 24 (2002) 411–433

JOURNAL OF STRUCTURAL GEOLOGY

www.elsevier.com/locate/jstrugeo

Deformation history of the Roanoke recess, Appalachians, USA

S. Alan Spraggins, William M. Dunne*

Department of Geological Sciences, University of Tennessee, Knoxville, TN 37996-1410, USA

Received 28 June 2000; accepted 3 May 2001

Abstract

The evolution of the Roanoke recess is controversial because agreement is lacking about the timing and continuity of deformation increments; because it may or may not have behaved like an adjacent salient and recess; because while many salients have been investigated, few recesses have; and because the role of blind thrusts is unclear. To gain insight into these controversies, we estimated shortening directions, shortening magnitudes and relative timing in the recess from map-scale folds, outcrop-scale stylolites, and grain-scale solution structures and twins. The key results from combining these new data with previous work are as follows. (1) The deformation history around the Roanoke recess is most simply described as temporally continuous with deformation migrating northeastward while the primary shortening direction rotated counterclockwise from N-directed to almost W-directed. (2) Consequently, the Roanoke recess did not deform in the symmetrical manner of the adjacent Pennsylvania salient nor with the two-step history of the Kingston recess further to the north in the Appalachians. (3) The timing and magnitude of shortening increments are sufficient to necessitate a blind thrust under the present surface rocks of the inner recess throughout the deformation history.

Keywords: Noncoaxial deformation history; Recesses; Salients; Appalachians; Limestones; Blind thrusts

1. Introduction

A recess is a map-view curve of structural trend in an orogenic belt that is concave toward the craton, while a salient is a convex curve toward the craton (Fig. 1). An important kinematic question for the evolution of recesses and salients is whether their curvature is the result of a pre-existing curve or the result of curvature imposed during orogeny. Recesses and salients with syn-orogenic curvature are oroclines and result from many different tectonic processes: oblique intersection of orogens, interaction of an orogen with obstacles in the foreland, horizontal rotation of crustal blocks, irregular continental margins, lateral variation in pre-deformational basin stratigraphy, lateral variation in orogenic taper, and interaction of an orogen with a pre-existing strike-slip fault (Carey, 1955; Ries and Shackleton, 1976; Thomas, 1977; Marshak and Tabor, 1989; Ferrill and Groshong, 1993a; Marshak and Flöttmann, 1996; Gray and Stamatakos, 1997; Hindle and Burkhard, 1999; Macedo and Marshak, 1999). These processes involve kinematic behaviors such as: bending, radial thrusting, parallel displacement paths, curve-parallel simple shear and two-step overprint (Fig. 1).

While the kinematic history and causative processes of many salients are well understood (e.g. Macedo and Marshak, 1999), the evolution of recesses has received very little direct investigation. Perhaps recesses form in a mirror manner to their adjacent salients, perhaps they do not. Marshak and Tabor (1989) did investigate the origin of a recess. Using crosscutting field relationships and strain measurements, they found a two-step deformation history where older structures rotated at an intersection orocline, the Kingston recess (Figs. 1 and 2). The structural history of this recess does not mirror the adjacent Pennsylvania salient where deformation was symmetrical and continuous in time (e.g. Nickelsen and Hough, 1967; Nickelsen, 1988; Nickelsen and Engelder, 1989; Evans, 1994; Spiker and Gray, 1997; Younes and Engelder, 1999).

We chose to examine the evolution of the Roanoke recess in the Appalachians because of the paucity of investigations of recesses, and because of the controversies concerning its evolution. The recess formed during the Alleghanian orogeny at a pre-existing promontory (Thomas, 1977; Hatcher et al., 1989) where surface thrust faults of the southern Appalachians meet surface macrofolds above duplexes of the central Appalachians (Fig. 2). One controversy is whether the Roanoke recess should be expected to have developed like the Kingston recess because it is in the same orogen, whether the Roanoke recess should be a mirror of the adjacent Pennsylvania salient, or whether the recess should have its own unique deformation history.

* Corresponding author. Tel.: +1-865-974-5498; fax: +1-865-974-2368.
E-mail address: wdunne@utk.edu (W.M. Dunne).

0191-8141/02/$ - see front matter
PII: S0191-8141(01)00077-3

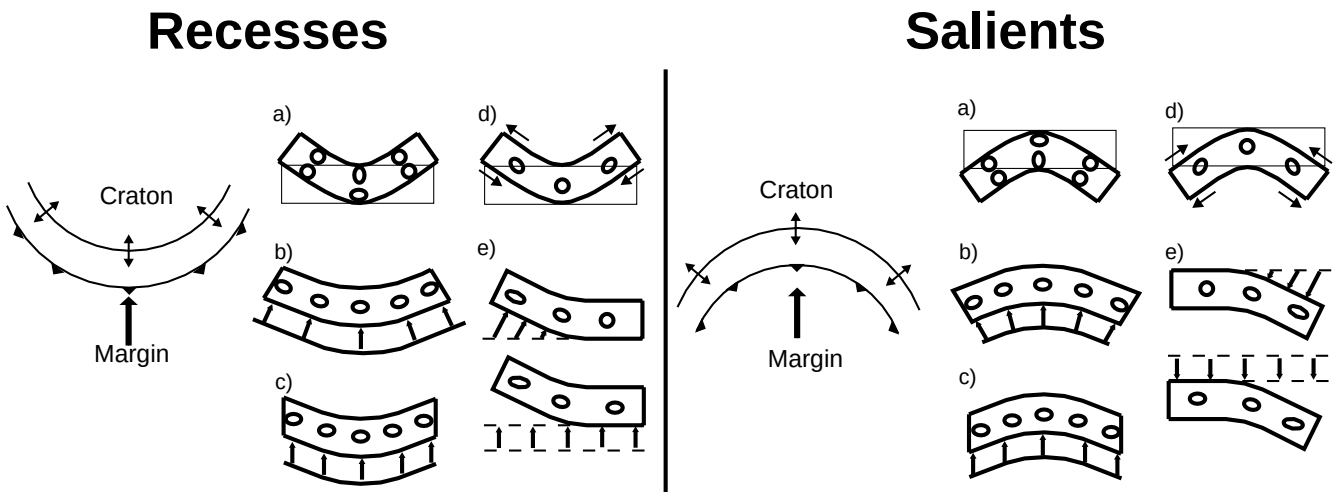

Fig. 1. Basic geometry and kinematic models for formation of recesses and salients (modified from Marshak, 1988; Ferrill and Groshong, 1993a). Basic geometry shows transport direction (arrow), structural trend and relative positions of craton and continental margins. Circles and ellipses show schematic strain distributions for kinematic models. (a) Bending, (b) Centripetal (recess) and radial (salient) displacement, (c) Parallel and equal displacements on a pre-existing curve, (d) curve-parallel simple shear, and (e) two-step history (thin-lined rectangles and dashed lines represent undeformed reference features).

Another controversy assumes that the recess has a two-step origin similar to the Kingston recess, so the question is whether southern or central Appalachian structures formed first at the recess. The prevailing view is that the southern structures are older (Rodgers, 1970; Dean et al., 1988). The evidence for this interpretation is that the youngest deformed strata in the southern Appalachian foreland are older than in the central Appalachian foreland (Rodgers, 1970); a map-scale fold interference pattern in the recess (Bick, 1986); and an early cleavage being related to southern Appalachian shortening (Dean et al., 1988). Recently, this prevailing view was challenged (Whitaker and Bartholomew, 1999) because the overturned limb of a large southern Appalachian fold was found to contain structures recording central Appalachian shortening trends when the effects of folding were removed. As a result, we evaluate the kinematic evolution of a thrust belt in the Roanoke recess, using the timing and deformation contributions of structures in the interior of the recess. We use the evaluation to address whether the Roanoke recess formed like the mirror of the Pennsylvania salient, like the Kingston recess or uniquely. We address relative timing issues of structures around the recess, and we consider the implications for the interaction between possibly emergent southern Appalachian thrusts and central Appalachian duplexes, which both have large displacements and are laterally continuous.

2. Geological setting and previous work

The study area is located in the Appalachian Plateau, which is in the inner arc of the Roanoke recess (Figs. 2 and 3). To the southeast, the Plateau is bounded structurally by the St. Clair thrust and the footwall Glen Lyn syncline of southern Appalachian origin trending 060° (Rodgers, 1970). To the east, it is bounded by the Wills Mountain anticline, which is over the blind Wills Mountain duplex of central Appalachian origin trending 025° (Perry, 1978; Wilson and Shumaker, 1992; Dunne, 1996). To the northwest beyond the study area, the Plateau is bounded by the North American craton (Muehlberger, 1992).

We divide the Plateau in the Roanoke recess into three structural domains (Fig. 2b) that have internally consistent macrostructural characteristics. The southern domain contains only structures with a southern Appalachian trend. The transitional domain contains folds with a central Appalachian trend at 030° but is bound to the southeast by a fold and thrust with a southern Appalachian trend. The northern domain contains only folds with central Appalachian trends.

2.1. Blind thrusts and the transition from the southern to central Appalachians

The northward transition from the southern to central Appalachians is marked by several changes in structural style (Rodgers, 1970; Woodward, 1985; Kulander and Dean, 1986; Onasch and Dunne, 1993). The structural trend changes from 055°–060° to 025°–030°. Presently emergent thrusts mostly with maximum displacements exceeding 20 km give way to map-scale folds above blind duplexes with displacements up to 20 km. Thrust sheets of rocks ranging in age from Cambrian to Mississippian give way to horses of Cambrian to Middle Ordovician rocks that underlie a decoupled roof sequence of Middle Ordovician to Mississippian rocks (Fig. 3). All of these changes occur in the Valley and Ridge, which is SE of the Plateau. An issue when examining deformation in the inner recess is the presence and geometry of these transitions in the Plateau.

Controversy exists as to the degree of involvement of

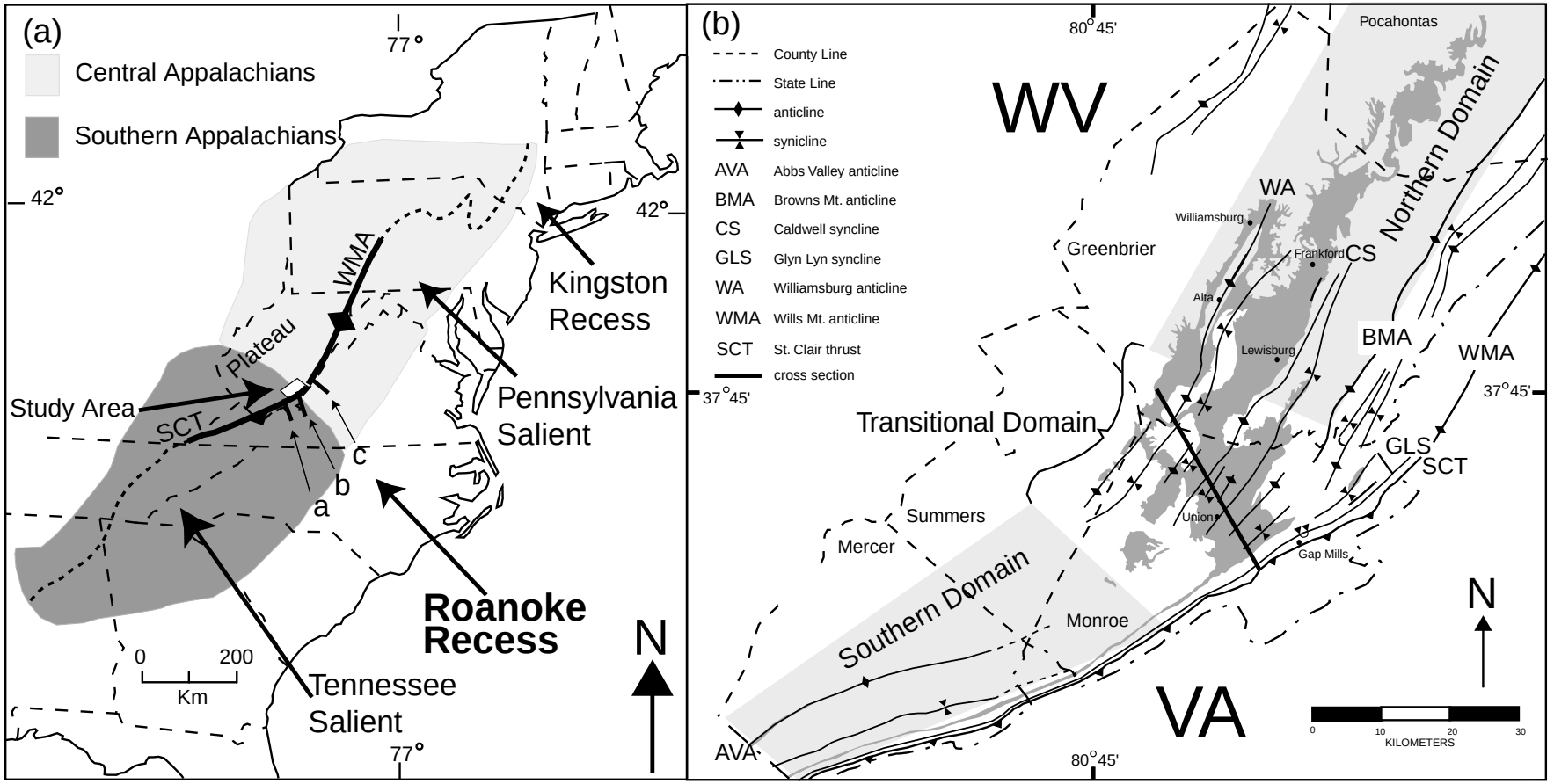

Fig. 2. (a) Locations of study area, and cross-sections in Fig. 3 with respect to salients and recesses in central and southern Appalachians. (b) Greenbrier outcrop belt (medium gray) in study area modified from Cardwell et al. (1968), cross-section line (Fig. 6) and major structures from Mercer to Pocohontas County, West Virginia. Structural domains across recess also shown using light gray.

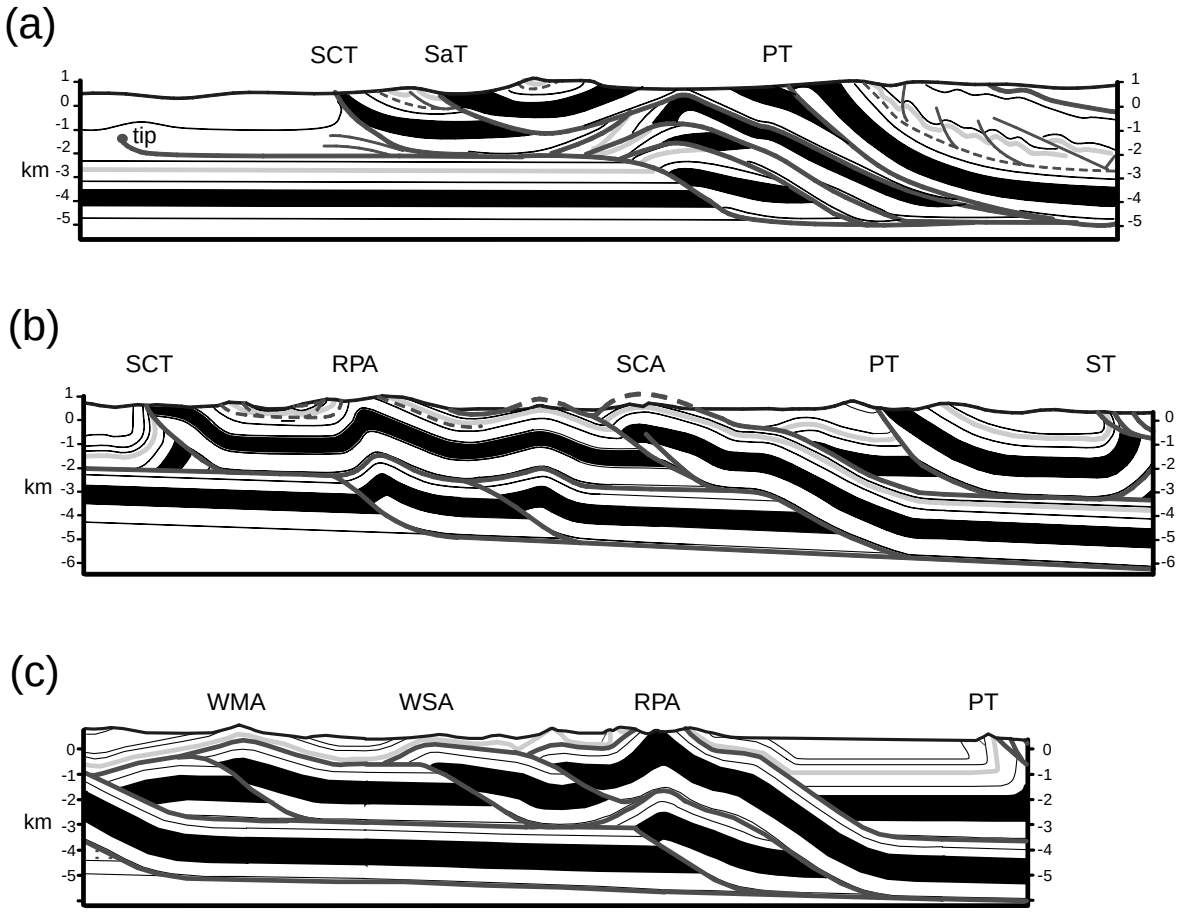

Fig. 3. (a) Cross-section for southern Appalachians (modified from Kulander and Dean, 1986). (b) Cross-section for transitional region (Onasch and Dunne, 1993) (c) Cross-section for central Appalachians (Couzens and Dunne, 1994). Section locations are shown in Fig. 2a. Solid black unit is the Cambro–Ordovician Knox Group or stratigraphic equivalent. NT—Narrows thrust; PT—Pulaski thrust; RPA—Rich Patch anticline; SCA—Sinking Creek anticline; SaT—Saltville thrust; SCT—Saint Clair thrust, ST—Salem thrust; WMA—Wills Mountain anticline; WSA—Warm Springs anticline.

Plateau rocks during central and southern Appalachian deformation. Workers agree that the Plateau in the recess was an area of active blind thrusting during the late Paleozoic formation of the central Appalachian portion (Fig. 3c) of the Alleghanian thrust belt (Gwinn, 1964; Kulander and Dean, 1986; Wilson and Shumaker, 1992). Blind thrust flats transferred displacement into the Plateau from the belt, forming the Browns Mountain anticline (BMA) above a duplex and also several detachment folds with central Appalachian trends. Most workers (Woodward, 1985; Kulander and Dean, 1986; Whitaker and Bartholomew, 1999) also believe that displacement from the southern Appalachian portion of the Alleghanian thrust belt was not substantially transferred into the Plateau. Instead, up to 20 km of thrust displacement for the southern Appalachian St. Clair thrust sheet emerges through the surface trace of the St. Clair thrust in front of the Plateau (Fig. 3a). Using this pair of interpretations, thin-skinned penetrative deformation in the Plateau should only be related to central Appalachian shortening because a significant blind flat was only operative in this area at that time.

An alternative hypothesis (Fig. 3b) is that the St. Clair thrust is only an imbricate fault of a blind thrust flat, which continues into the Plateau (Couzens and Dunne, 1994). If true, thin-skinned penetrative deformation could occur in this area throughout development of the Alleghanian thrust belt because a blind thrust flat was operative at all times. In this case, the Plateau could have experienced either continuous or episodic deformation during blind thrust accommodation for both the formation of the southern and central Appalachian portions of the Alleghanian thrust belt. Previous work (Dean et al., 1988) has documented that Plateau rocks experienced shortening during formation of southern Appalachian structures and we intend to measure shortening magnitudes and directions to determine the amounts and relative timing of shortening events in the recess interior. We believe that a continuity of behavior through time would indicate that displacement transfer is occurring from a blind thrust that was active during the movement of both the St. Clair thrust sheet of the southern Appalachians and the blind Wills Mountain duplex of the central Appalachians. Such an interpretation logically leads to the conclusion that these two large structures, which both have about 20 km of displacement are

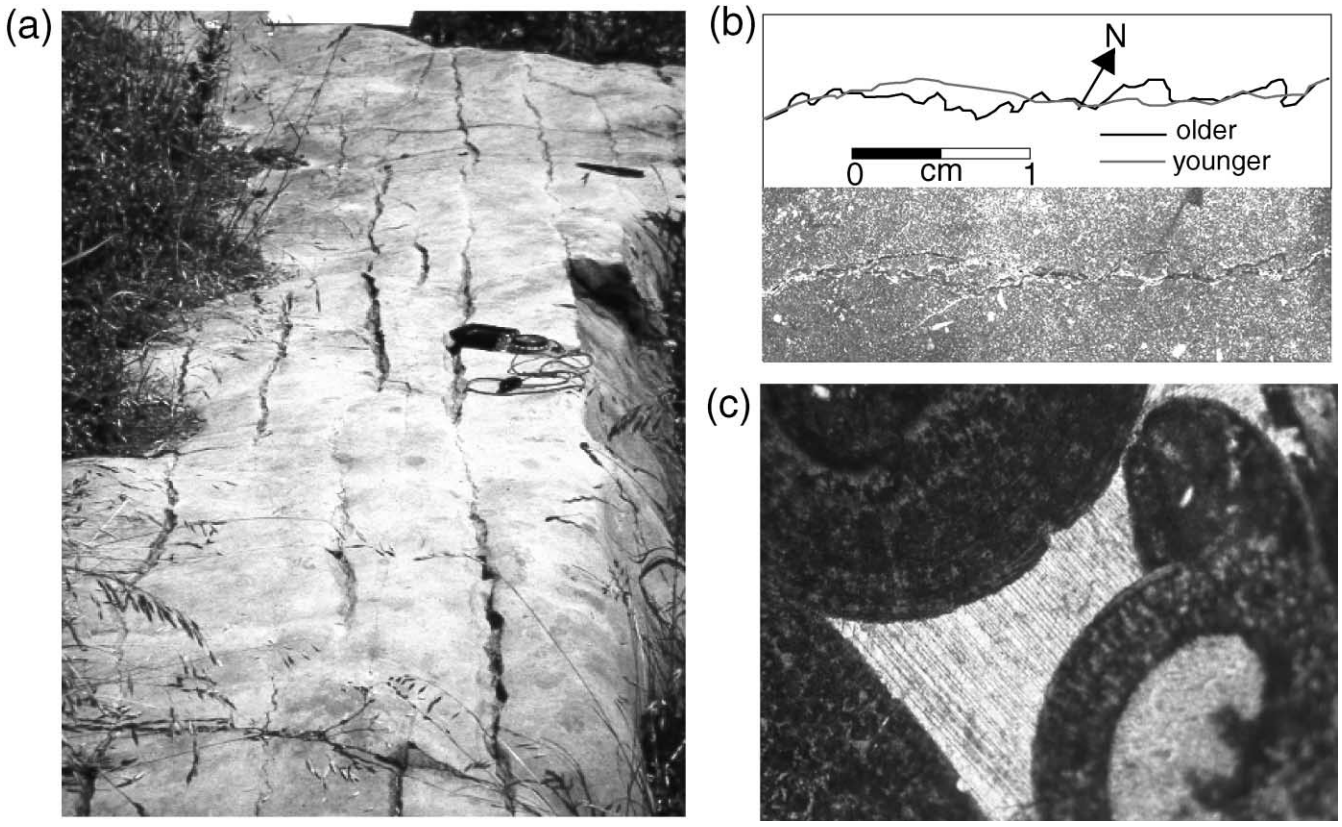

Fig. 4. Greenbrier bedding pavement with bed-normal stylolitic cleavage (Silva Ranger™ compass for scale). (b) Cross-cutting stylolites from station J1 with interpretation above photograph. (c) Twinned calcite cement grain between interpenetrating ooid grains that are evidence for grain-to-grain dissolution (photo 1 mm wide).

laterally continuous (Wilson and Shumaker, 1992; Couzens and Dunne, 1994).

2.2. Target stratigraphic unit

In this study, we use limestones of the Upper Mississippian Greenbrier Group (Reger and Price, 1926; Ogden, 1976; Skinner, 1979) (Figs. 4 and 5) because: (1) limestone is probably the most effective sedimentary rock for investigating low-intensity meso- and microscale deformation (Cloos, 1947; Groshong, 1972; Marshak and Engelder, 1985; Schmid et al., 1987; Groshong, 1988; Protzman and Mitra, 1990; Smart et al., 1997); (2) calcite deforms by twinning, fiber growth and solution (Fig. 4), providing partial and finite strains (Groshong, 1972; Powell, 1979; Marshak and Engelder, 1985; Meyer and Dunne, 1990); and (3) the unit has abundant outcrops in the inner arc of the recess. Unit thickness averages about 340 m in the study area, consists of six major formations (Fig. 5), is conformably overlain by the Mississippian Mauch Chunk Group, and underlain by the Mississippian McCrady Formation. The primary lithology for this investigation is ooid grainstone (Dunham, 1962), although some stylolitic shortening values were measured in packstones. This sampling restriction was used to eliminate lithology as a variable when analyzing structures in different locations.

3. Macroscale shortening

A geologic cross-section was constructed to estimate macroscale shortening for the Greenbrier Group in the Plateau beyond the St. Clair thrust (Figs. 2b and 6). Previous mapping in the area (Reger and Price, 1926; Ogden, 1976; Skinner, 1979) supplemented structural and stratigraphic data from this study. The cross-section line was positioned in the center of the recess near the termination of map-scale central and southern Appalachian folds. The section was constructed along 150–330°, which is normal to the southern Appalachian structural trend so as to be able to integrate the shortening contribution of smaller structures in this direction. While not all structures along this section are of southern Appalachian origin or geometry, the section is being used to resolve shortening components of the structures parallel to a normal to the southern Appalachian trend. The section is not an attempt at a restoration or 'balancing'.

The transect crosses 11 folds from the overturned Glenn Lyn syncline in the SE to the Williamsburg anticline in the NW. The folds are shown as open folds with straight limbs

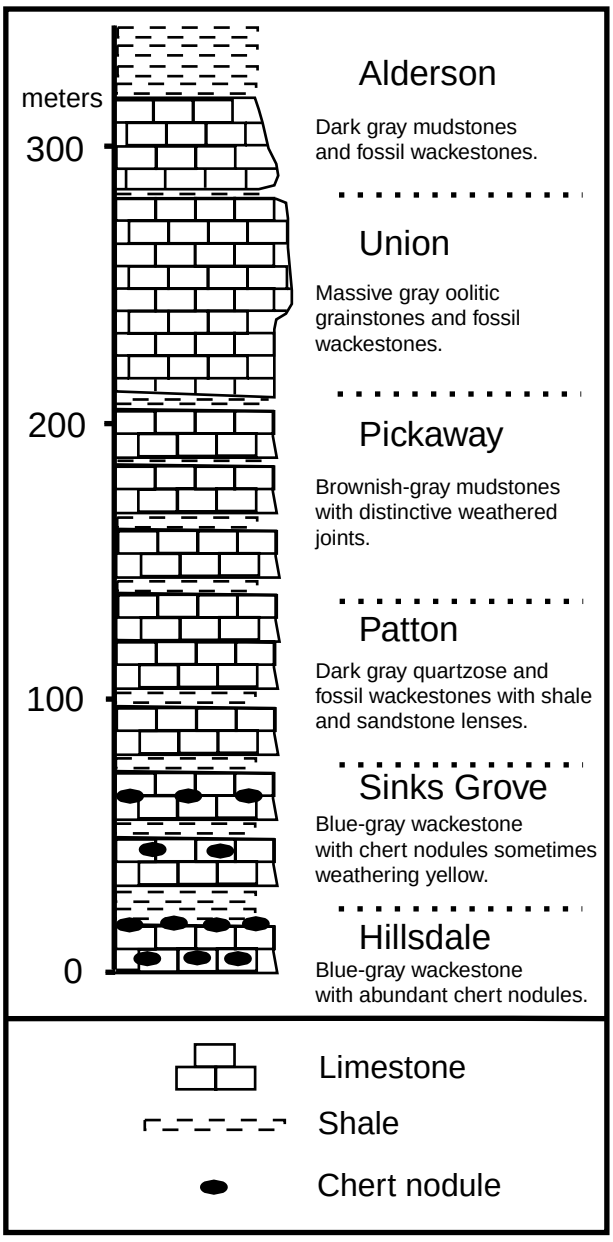

Fig. 5. Stratigraphic column for the Mississippian Greenbrier Group in Monroe County, West Virginia (modified from Reger and Price, 1926; Price, 1929; Price and Heck, 1939; Ogden, 1976; Skinner, 1979).

and constant layer-normal thickness, based on field observations of fold shapes and preservation of layer thickness through folds (Fig. 6). Also, map-scale faults are absent from the Greenbrier Group in the cross-section as they were not found during mapping in the study area.

The component of macroscale shortening parallel to the section within the Greenbrier Group was measured as a line length change (Dahlstrom, 1969), because bed thicknesses are constant and interpreted to be preserved in rock exposures. An initial bed length of 28.3 km and a final bed length of 27 km yields 1.3 km or 4.7% macroscale section-parallel shortening by a combination of folds with central and southern Appalachian trends (18% southern and 82% central trends, respectively).

4. Strain assessment

4.1. Greenbrier cleavage shortening

Limestones of the Mississippian Greenbrier Group are well exposed throughout the study area (Figs. 2b and 4a). Outcrop-scale folds and faults are almost completely absent in the Greenbrier Group at the ground surface. Instead, the dominant outcrop-scale structure is cleavage (Dean et al., 1988).

Cleavage morphology within the Greenbrier Group is dependent on lithology. Cleavage in wackestones and mudstones (Dunham, 1962) is typically smooth and parallel but sometimes anastomosing (Powell, 1979). Packstones have smooth to stylolitc cleavage. Grainstones commonly have stylolitic cleavage. Cleavage truncates bedding laminations, and clay is preferentially concentrated in the cleavage zones. Bedding-cleavage intersection or dihedral angles typically exceed 85°, indicating a bed-normal geometry. Previous work (Dean et al., 1988) identified a complex array of multiple layer-parallel shortening directions from stylolitic column geometries across the region (Fig. 7). These workers did not identify the relative ages of the shortening directions on the basis of crosscutting cleavage geometries, nor did they estimate shortening magnitudes. As a result, the grainstones and packstones with stylolitic cleavage were re-examined to: (1) review the number and array of layer-parallel shortening directions; (2) determine relative age of shortening directions from crosscutting relationships; and (3) estimate shortening magnitudes from column amplitudes (Smart et al., 1997).

Shortening magnitude estimates for the cleavage were obtained from scanlines parallel to the stylolite teeth orientation on bedding, because this trend represents the actual shortening direction (Fig. 8). A minimum of three scanline measurements were taken for each station as a test for consistency. Shortening was calculated as an elongation (Means, 1976, p. 135) where the final length is the length of the scanline and the initial length is the final length plus the sum of the stylolite amplitudes. This technique assumes that the amplitude of the stylolite teeth represents the width of dissolved material, which is a minimum estimate of shortening because volume loss could have occurred without increasing stylolite amplitude (Geiser and Sansone, 1981). This assumption of minimum shortening is a premise of the original solution explanation for stylolite formation (Stockdale, 1922, p. 59), is consistent with the anticrack hypothesis (Fletcher and Pollard, 1981), and is consistent with an independent measure of strain versus size of teeth (Alvarez et al., 1978).

If the assumption is incorrect, what would be the impact? The technique would still yield a relative measure of

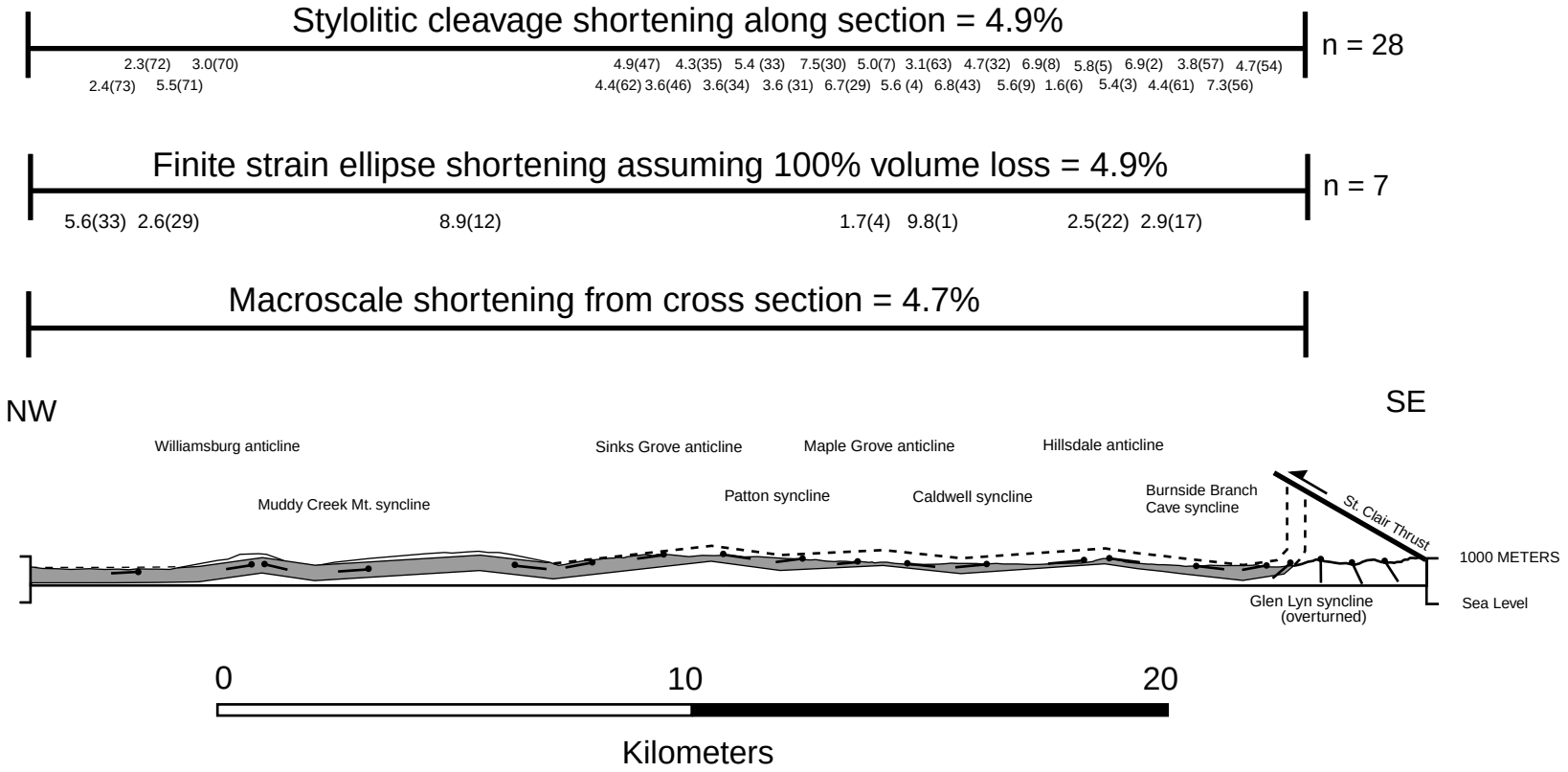

Fig. 6. Cross-section of Mississippian Greenbrier Group (gray) shown with a thickness of 340 m (Reger and Price, 1926; Ogden, 1976; Skinner, 1979). Also shown are contributions to total shortening from measurements of cleavage and Fry analyses (see Tables 1 and 3).

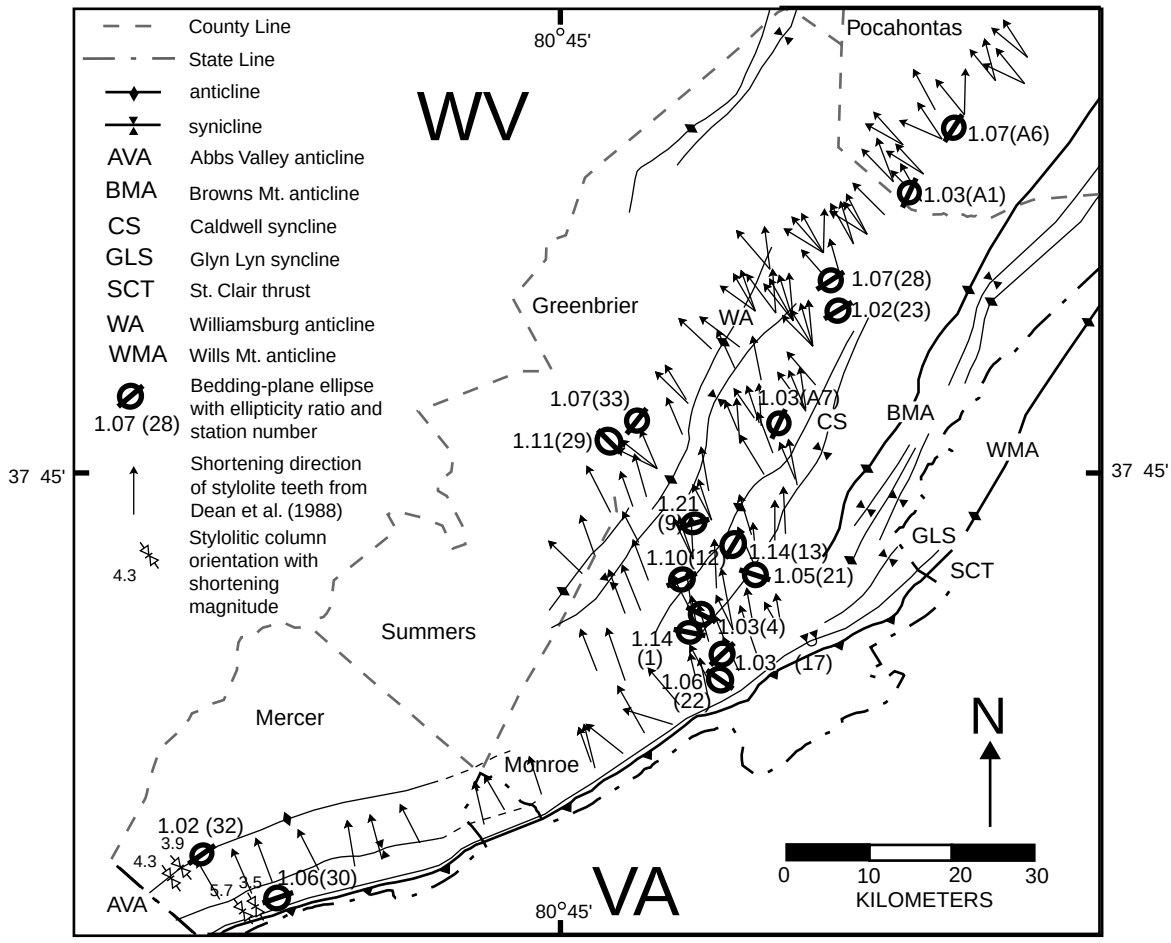

Fig. 7. Map showing bedding-plane strain ellipses for whole study area (Table 3), cleavage shortening values of the southern domain from this study (Table 1), and cleavage shortening directions from Dean et al. (1988).

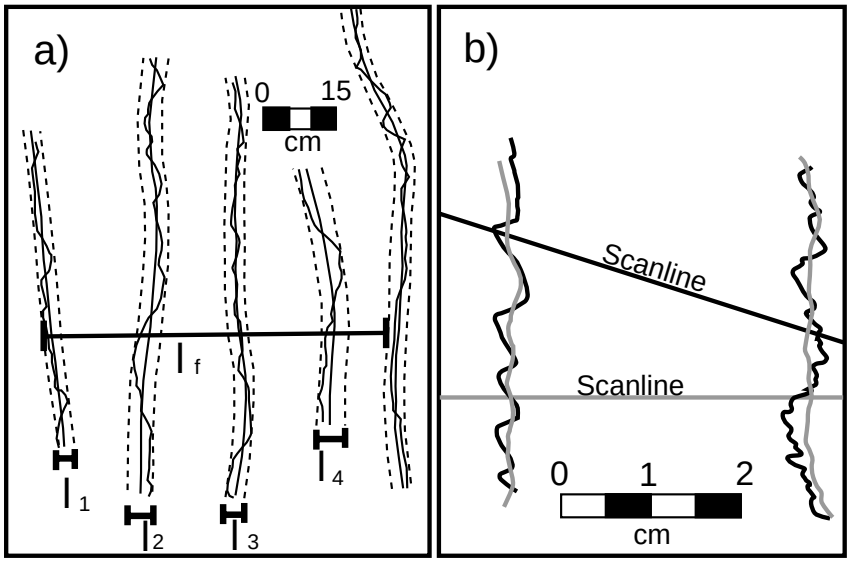

$$l_i = l_f + l_1 + l_2 + l_3 + l_4$$

Fig. 8. (a) Schematic representation of shortening measurements from stylolitic cleavage traces on a bedding surface (modified from Smart et al. (1997). (b) Scanlines oriented parallel to stylolite column orientation (black — older traces, gray — younger traces).

shortening from station to station for the same pressure–temperature conditions in the same lithology, which would be informative. The measured values would be underestimates because they are minimum estimates, so outcrop-scale shortening due to cleavage would be even greater, which would be favorable to subsequent interpretations in this paper. Given the lack of an independent check to prove/disprove the assumption, given the lack of damaging result if it is incorrect, and given the fact that the technique yields direct reproducible results from field measurements, we assume that the amplitude of stylolite teeth represents the width of dissolved material.

4.1.1. Results

Four stylolitic-column measurements from the southern domain show shortening oriented from 319 to 330°, subnormal to the host southern Appalachian folds, with an average of 324 ± 5° (Table 1, Fig. 7). Shortening magnitudes range from 3.5 to 5.7%, averaging 4.3 ± 1%.

Fifty-nine cleavage measurements from the transitional domain were separated into three groups of similar shortening directions (Table 1, Fig. 9). No measured shortening directions lie in the range of 290–300°, which would be expected if a true central Appalachian shortening direction was recorded. Instead, 66% (39 measurements) of the data lie between 300 and 320°, intermediate in orientation to the southern and central shortening directions. The average of these data trend 313 ± 6° with shortening magnitudes of 0.6–8.3% that average 4.4 ± 2%. Only three measurements have shortening oriented near the typical southern Appalachian direction 330° with values of 321–340°. The remaining 29% (17 measurements) of the data indicate shortening oriented more northerly than the typical southern Appalachian shortening direction. These data average a trend of 353 ± 5° with shortening magnitudes of 1.2–7.4% that average 4.7 ± 2%.

The 29 cleavage measurements from the northern domain (Table 1, Fig. 9) have shortening trends (300–330°) that are intermediate between the central Appalachian shortening direction (295–300°) and the southern Appalachian shortening direction (325–330°). Fifty-nine percent (17 measurements) of the data fall between 310 and 320°, and overall, the 29 measurements average a trend of 318 ± 7°. Shortening magnitudes range from 1.7 to 10.7% with an average of 5.8 ± 3%.

As recognized by Dean et al. (1988) (Fig. 7), the stylolitic cleavage shows a more complex array of trends (strikes) when compared with the simpler set of just two trends for map-scale structures. However, unlike Dean et al. (1988), we found the complexity only occurs in the transitional zone. Stylolites in the southern domain are consistently parallel with the map-scale folds and faults (Fig. 7). Stylolitic cleavage of the northern domain has only one trend with one dominant shortening direction of 318°, which is not normal to map-scale structures (Fig. 9). In contrast, the stylolitic cleavage in the transitional domain records two dominant shortening directions and neither are normal to the trends of either central or southern Appalachian map-scale structures. Instead, they are parallel to an intermediate direction of 313° and an almost N–S trend of 353°.

4.1.2. Crosscutting cleavage

Given the variety of shortening directions recorded by stylolites in the transitional domain, determining their age relationships would ideally be achieved by comparing the different stylolites and teeth orientations at the same exposure. As it turns out, the only relative age data come from examining a single set of stylolites that has the unusual morphology of teeth overprinting teeth. Evidence for a deformation sequence was obtained for crosscutting stylolitic columns along the same cleavage surfaces (Figs. 4b and 10). Seven oriented samples with this morphology were collected for stylolite surfaces trending 042–050° (Figs. 10 and 11). The samples were cut into slabs and polished to reveal and verify the morphology, because it is very difficult to identify in the field (Figs. 4b and 10). The set of surfaces with the asymmetric columns is much more noticeable with a thick clay selvage and shortening magnitudes averaging around 3.5% with a column trend of 342 ± 9°. The other set of surfaces with more symmetric columns has less clay and a smaller shortening magnitude averaging less than 2% with a column trend of 322 ± 4°. In all cases, sinuous traces of the second set of teeth cut through the first set and hence, are younger, indicating that the northerly shortening direction is older.

Also, sets of stylolitic cleavage trending 060–075° and 030–045° are present in the same outcrops in the transitional domain. Dean et al. (1988) interpreted these sets to result from coaxial deformation by the stylolitization of pre-existing joint surfaces. We also found both sets to share one orientation for teeth of 350–360°, indicating that they are the same age.

4.2. Calcite twins

The calcite strain-gauge technique was used to calculate twinning strains in about 25 grains from each of two mutually perpendicular sections for 12 samples (Table 2, Figs. 4c and 12). Calculations used the inner twin width for thick twins and a twinned material ratio of 0.5 for thin twins (Groshong, 1972, 1974; Groshong et al., 1984a; Evans and Groshong, 1994). Measurement precision and accuracy were improved by discarding 20% of the twin sets with the largest deviation (LDR, Table 2) from the calculated strain tensor, minimizing measurement errors (Groshong, 1974; Groshong et al., 1984a,b; Ferrill, 1991; Ferrill and Groshong, 1993a,b).

The total distortion for twinned samples varies from 0.2 to 3.1%, and averages 1.0 ± 0.9%. Distortion magnitudes are quite comparable with magnitudes determined from twins in the Greenbrier Group samples gathered about

Table 1
Stylolitic cleavage data

Station number	Bedding orientation	Cleavage unrotated[a]	Cleavage rotated[b]	Teeth orientation (°)	Number of traces	Average column amplitude (cm)	Scanline length (cm)	Percent shortening
Stylolitic cleavage data for southern domain								
113	057/60	065/30	053/90	323	6	1	100	5.7
114	060/62	059/25	060/87	330	6	0.6	100	3.5
115	059/60	070/23	055/83	325	9	0.5	100	4.3
116	059/60	078/33	229/88	319	5	0.8	100	3.8
Average:				324 ± 5				4.3 ± 1%
Stylolitic cleavage data for transitional domain with shortening oriented 300–320								
1	051/09	221/82	222/81	312	13	0.35	50	8.3
2	159/13	037/90	218/83	308	10	0.8	100	7.4
3	161/06	041/83	041/86	311	10	0.6	100	5.7
5	162/08	214/88	214/83	304	14	0.5	100	6.5
6	174/03	047/87	047/89	317	5	0.2	60	1.6
8	184/09	052/78	051/84	320	5	0.3	20	7
9	180/08	050/82	049/87	319	6	0.5	50	5.7
22	029/03	213/82	213/85	303	8	0.1	35	2.2
23	033/05	215/80	215/85	305	5	0.5	50	4.8
24	308/07	044/80	045/81	315	4	0.4	75	2.1
32	115/07	228/86	228/89	318	4	1	80	4.8
36	222/14	032/90	032/90	302	10	0.3	80	3.6
37	122/10	034/82	033/82	303	3	1	60	4.8
38	122/10	038/84	037/83	307	2	1.5	50	5.7
39	210/16	038/70	038/86	308	13	1	200	6.1
40	215/18	036/82	216/80	306	6	1	100	5.7
41	030/28	210/79	030/73	300	4	0.4	50	3.1
42	068/16	038/68	040/82	310	3	0.3	50	1.8
43	198/18	048/80	228/84	318	3	1	40	7
48	216/08	045/84	225/88	315	9	1	100	8.3
49	205/05	050/82	050/87	320	10	0.8	100	7.4
52	044/10	224/82	044/88	314	11	0.5	100	5.2
54	255/06	048/65	049/70	319	3	1	60	4.8
55	245/05	045/70	046/75	316	9	0.8	100	6.7
56	248/06	048/72	049/78	319	8	1	100	7.4
63	225/20	045/80	225/80	315	2	0.5	30	3.2
66	238/20	225/66	226/86	316	4	0.5	60	3.2
67	240/20	225/74	222/55	312	6	0.4	50	4.6
70	209/23	225/76	045/82	315	4	0.4	50	3.1
71	030/03	045/90	045/90	315	2	0.3	10	5.7
72	028/16	227/78	047/87	317	5	0.3	60	2.4
73	184/06	050/90	230/86	320	2	0.5	40	2.4
83	040/05	045/90	045/85	315	3	0.8	60	3.8
84	048/17	047/73	047/90	317	2	0.4	40	2
86	194/18	082/90	263/83	315	1	0.6	60	1
88	158/19	082/90	081/85	320	1	0.6	60	1
90	026/06	080/90	080/86	320	1	0.6	100	0.6
92	066/06	080/90	080/84	320	1	0.6	100	0.6

Table 1 (*continued*)

Station number	Bedding orientation	Cleavage unrotated[a]	Cleavage rotated[b]	Teeth orientation (°)	Number of traces	Average column amplitude (cm)	Scanline length (cm)	Percent shortening
93	240/08	040/90	220/82	310	7	0.5	100	3.4
Average:				313 ± 6				4.4 ± 2%
Stylolitic cleavage data for transitional domain with shortening oriented 330–340								
4	161/06	215/90	215/86	340	12	0.5	100	5.7
57	255/06	060/80	060/86	330	4	0.5	50	3.8
89	026/06	222/73	222/79	340	5	0.8	100	3.8
Average:				337 ± 6				4.5 ± 1%
Stylolitic cleavage data for transitional domain with shortening oriented 341–360								
7	184/09	122/86	121/82	350	5	0.5	45	5.3
16	155/07	035/87	215/89	345	6	0.5	50	5.7
21	145/22	042/81	040/86	344	6	0.3	90	2
29	226/13	037/78	217/89	355	8	1	100	7.4
30	226/13	037/78	217/89	355	9	1	100	8.3
31	066/07	038/90	038/90	350	5	0.8	100	3.8
33	060/05	040/90	040/90	350	6	1	100	5.7
34	060/05	045/90	045/90	350	5	0.8	100	3.8
35	060/05	045/90	045/90	350	6	0.8	100	4.6
46	264/14	040/86	220/84	360	3	1	70	4.1
47	198/10	054/90	054/90	360	3	1.2	60	5.7
61	054/06	044/90	044/84	360	2	0.8	30	5.1
62	260/11	046/90	226/81	355	4	0.5	40	4.8
85	194/18	224/74	043/90	354	3	0.8	60	3.8
87	158/19	043/90	224/82	355	3	1	60	4.8
91	066/06	222/83	222/88	350	4	1	100	3.8
94	240/08	087/90	267/83	357	2	0.6	100	1.2
Average:				353 ± 5				4.7 ± 2%
Stylolitic cleavage data for northern domain with shortening oriented 300–330								
10	214/51	210/33	212/84	302	3	0.2	35	1.7
12	210/11	226/83	227/72	317	9	0.5	50	8.3
13	202/03	050/83	050/86	320	7	0.6	40	9.5
15	200/10	045/80	045/89	315	8	1	100	7.4
74	038/10	226/78	226/88	316	5	0.3	60	2.4
76	010/16	047/69	045/82	315	5	0.8	80	4.8
77	022/18	049/74	048/90	318	4	0.8	80	3.8
78	028/05	048/90	048/85	318	7	0.2	40	3.4
79	018/09	046/90	046/82	316	3	0.4	50	2.3
80	016/12	048/62	045/72	315	2	0.5	30	3.2
81	240/10	222/72	043/82	313	2	1	50	3.8
95	355/04	225/78	224/81	330	9	0.5	100	4.3
96	355/04	080/90	080/90	330	8	0.8	100	6
97	200/04	042/78	042/82	312	9	0.5	100	4.3
98	210/06	056/82	056/87	326	6	1.5	100	8.3
99	210/08	054/80	054/87	324	7	1	100	6.5
100	205/05	040/80	040/85	310	6	1.2	100	6.7

Table 1 (*continued*)

Station number	Bedding orientation	Cleavage unrotated[a]	Cleavage rotated[b]	Teeth orientation (°)	Number of traces	Average column amplitude (cm)	Scanline length (cm)	Percent shortening
101	204/06	054/75	053/80	323	8	1.4	100	10.1
102	200/06	052/81	052/86	320	8	1	100	7.4
103	208/05	048/84	048/89	330	10	1	100	9.1
104	205/05	045/78	045/83	315	5	1.2	50	10.7
105	210/08	042/80	042/88	312	6	0.8	50	8.8
106	204/06	050/84	050/89	320	8	1	100	7.4
107	200/05	048/82	048/86	318	6	0.8	100	4.6
108	200/09	054/82	054/89	324	9	0.5	100	4.3
109	206/05	055/78	055/82	325	7	0.9	100	5.9
110	206/05	046/76	046/81	316	5	0.5	50	4.8
111	202/06	042/75	042/81	312	6	0.6	100	3.5
112	208/10	038/79	038/89	308	5	0.8	100	3.8
Average:				318 ± 7				5.8 ± 3%

[a] Indicates orientation with bedding.
[b] Indicates orientation after bedding is rotated to horizontal.

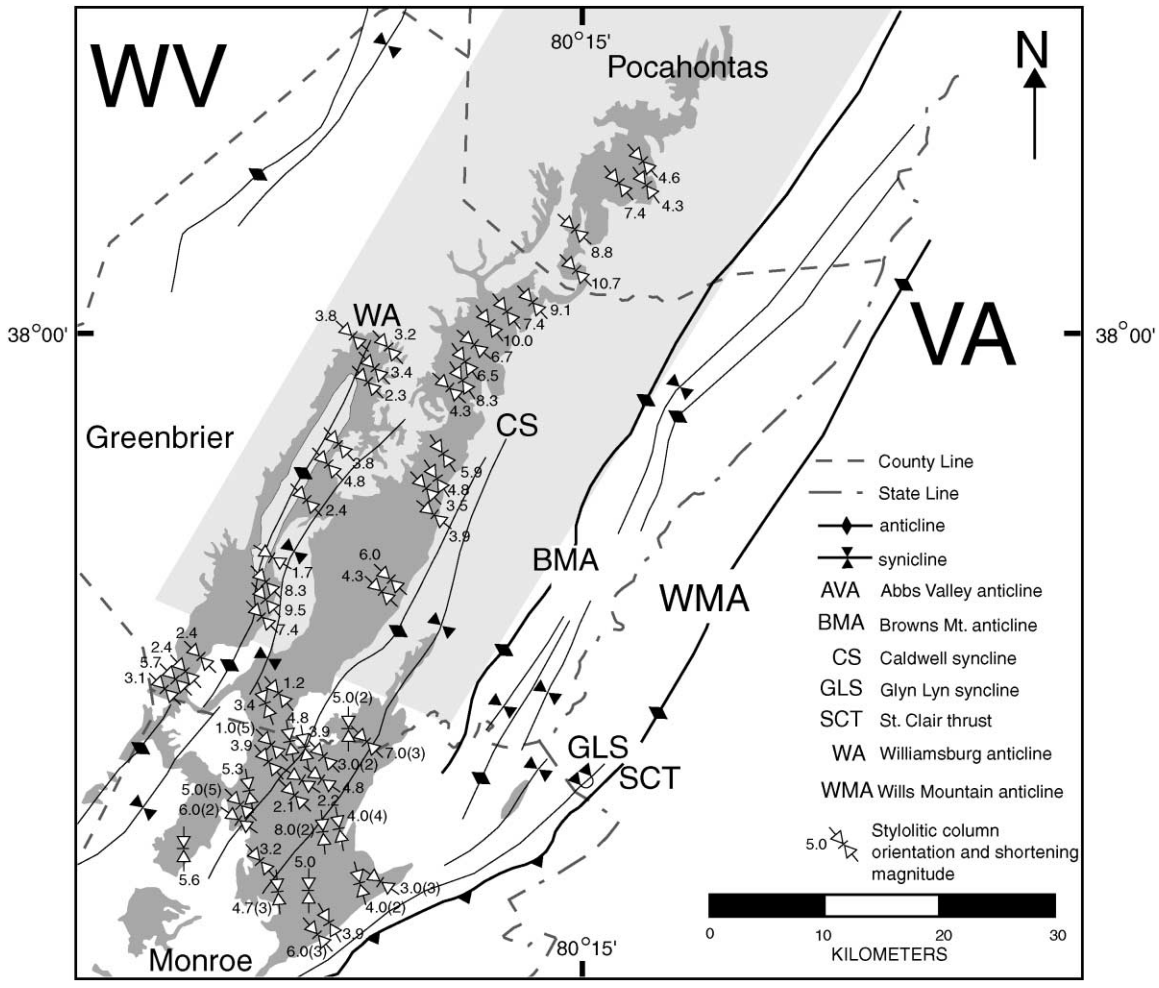

Fig. 9. Map showing stylolitic column orientations and estimated shortening magnitudes across cleavage. Number in parentheses is number of sample sites for an average value. Greenbrier outcrop shown in dark gray, transitional domain shown in white, and northern domain shown in medium gray (see Table 1).

70 km to the north, where the rocks only record central Appalachian deformation (Smart et al., 1997).

In the northern domain, the three twin samples have an average shortening direction (e_3 axial directions) of $308 \pm 10°$ (Table 2, Fig. 12). This trend is subnormal to fold axes with central Appalachian trends.

The transitional domain contains three distinct populations of orientations for e_3 axes (Table 2, Fig. 12): $359 \pm 23°$ (six samples), an E–W trend (two samples), and a NW–SE trend (two samples). Thus, the calcite twins record the same complexity of shortening directions (e_3 directions) that were interpreted from the columns of the stylolitic cleavage samples in the transitional domain (Tables 1 and 2, Figs. 9, 11 and 12). N–S and NW–SE shortening directions are present and are oblique to both the southern and central Appalachian shortening directions. In addition, the twins record a nearly E–W shortening direction that is absent in the measured cleavage data, but was locally recorded by Dean et al. (1988) in this domain.

As strain markers for a specific deformation mechanism, twins record very small deformations for low temperatures, stresses and differential stresses (Burkhard, 1993). They also record orogenic deformation well beyond the limits of a thrust belt (Craddock and van der Pluijm, 1989). So, different twins in the same sample could record components of both southern and central Appalachian shortening (Groshong, 1972, 1974; Burkhard, 1993). If so, these components might be separated by examining negative expected values (NEV) and positive expected values (PEV) for each sample set of twins. When e_3 axes are plotted for the twin samples from this study area for the NEV populations of the samples, they show no clear pattern (Fig. 13a). This result is perhaps not surprising as the NEVs are measurements that least fit the calculated ellipsoid for the entire sample population of twins, rather than having a characteristic shortening direction or magnitude. Given that these twin measurements are collected in an area with a known noncoaxial history, this result supports the reservations of Burkhard (1993) about attempting to separate different shortening events from calcite twins, using filters such as NEVs.

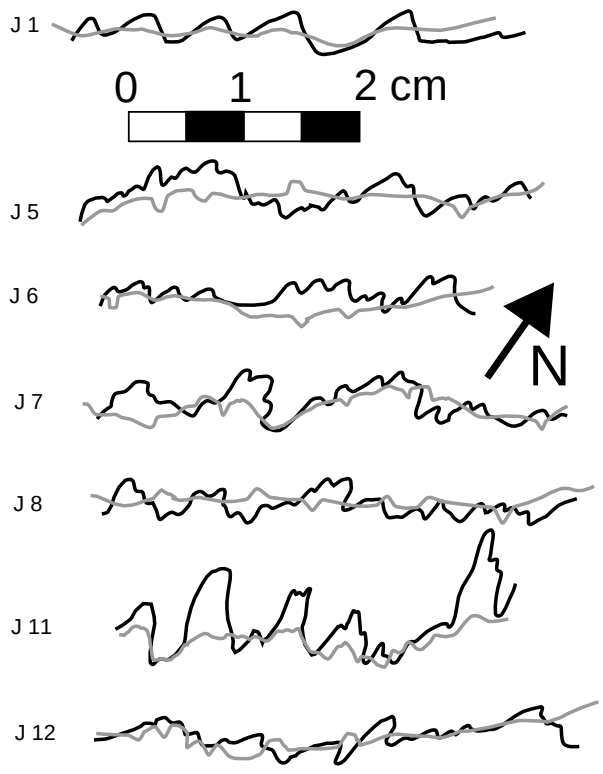

Fig. 10. Diagram example of crosscutting stylolitic cleavage morphologies from seven oriented samples. The black lines represent the first cleavage and gray lines are the second cleavage.

4.3. Fry analyses

Three mutually perpendicular thin sections were prepared from each of 17 oriented ooid grainstone samples for application of the normalized Fry method (Fry, 1979; Erslev, 1988). Enlarged photomicrographs of each thin section were digitized for ooid grain boundaries using software developed by W.A. Yonkee (pers. commun.). Finite strain ellipses were determined from measurements of 250 boundaries for each section and finite strain ellipsoids were calculated for each sample (Owens, 1984).

The strains were measured in rock volumes between the outcrop-scale stylolites but where twins are present. Consequently, these strains record the effects of deformation in the stylolite microlithons and include calcite-twin strains (Fig. 4c). Ideally, the shortening measured for the stylolitic cleavage and shortening magnitudes from the *R* values of the strain ellipses from the normalized Fry measurements could be added to characterize the total strain from cleavage development and internal microlithon deformation.

Principal shortening axes (*Z*) for the strain ellipsoids are nearly bed-normal in 14 of 17 samples, while the *Z* axes are nearly bed-parallel in two of the other three samples (Fig. 13b). Bedding-perpendicular thin-sections from all the samples exhibit bedding-parallel transgranular pressure-solution seams and sutured grain boundaries indicative of pretectonic vertical compaction, which is consistent with

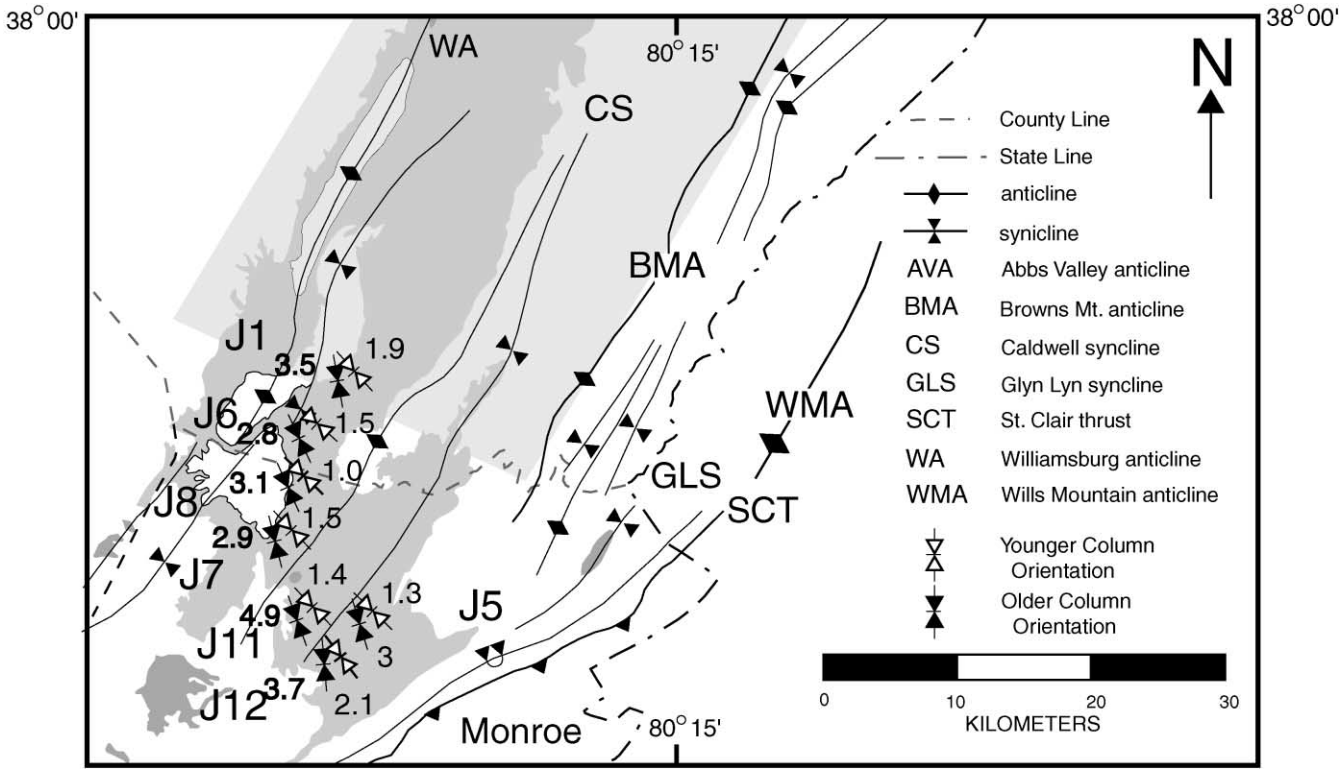

Fig. 11. Map showing difference in shortening directions and estimated shortening magnitudes for sample locations with crosscutting stylolitic teeth. Greenbrier outcrop in dark gray, transitional domain in white, and northern domain in medium gray. J values are station numbers (see Fig. 10).

Table 2
Calcite twin data

Sample bedding	Cleaning procedure[a]	Number of twin sets	Principal strains (% elongation)			Principal axis orientations[b]			Nom. error in strain	Percent NEV	Avg. width (mm)	Avg. intensity (twin/mm)	Total distortion (% strain)	Domain
			e_1	e_2	e_3	e_1	e_2	e_3						
1	n.a.	50	5.9	−1.0	−4.9	337/83	119/05	209/4	0.88	12	0.67	94	5.4	
010/12NW	LDR	40	2.3	1.2	−3.5	307/71	120/18	210/2	0.48	17.5	0.56	82	3.1	T
3	n.a.	49	2.9	0.3	−3.2	251/75	70/15	160/00	0.37	20.4	0.69	59	3.1	
034/24NW	LDR	40	2.3	0.2	−2.5	253/62	072/28	162/00	0.34	10	0.56	55	2.4	T
9	n.a.	50	1.1	−0.1	−1.0	062/28	197/54	320/22	0.2	22	0.32	44	1.1	
030/58NW	LDR	40	0.5	0.0	−0.5	063/38	213/48	321/15	0.09	12.5	0.17	39	0.6	T
11	n.a.	50	1.4	0.2	−1.6	167/79	341/11	071/01	0.17	36	0.38	50	1.5	
058/20NW	LDR	40	0.8	0.2	−1.0	143/81	350/08	259/04	0.17	25	0.27	46	0.9	T
12	n.a.	49	0.6	0.4	−1.0	269/76	092/14	002/01	0.34	26.5	0.29	61	0.9	
159/13SW	LDR	40	0.5	0.1	−0.6	283/61	091/28	185/07	0.15	37.5	0.16	55	0.6	T
17	n.a.	50	1.5	0.2	−1.7	139/05	246/75	047/14	0.33	8	0.29	77	1.6	
046/14SE	LDR	40	0.9	0.0	−0.9	146/12	268/69	049/16	0.11	7.5	0.17	69	0.9	T
21	n.a.	49	1.2	0.1	−1.3	079/87	286/12	196/01	0.19	28.6	0.29	52	1.2	
108/07NE	LDR	40	0.7	0.2	−0.9	059/83	285/05	195/05	0.09	22.5	0.17	49	0.8	T
22	n.a.	49	1.0	0.4	−1.4	112/73	283/16	013/03	0.16	4.1	0.27	66	1.2	
046/16SE	LDR	40	0.4	0.1	−0.5	103/16	266/73	011/05	0.07	0	0.14	58	0.5	T
29	n.a.	50	0.9	0.3	−1.2	058/66	270/21	175/12	0.27	30	0.27	65	1.1	
134/20SW	LDR	40	0.4	0.2	−0.6	067/45	276/41	172/15	0.1	20	0.14	63	0.6	T
33	n.a.	50	1.5	−0.2	−1.3	283/69	060/15	154/13	0.25	24	0.27	71	1.4	
136/20SW	LDR	40	0.9	−0.2	−0.7	271/61	048/22	145/18	0.11	25	0.15	65	0.8	T
A1	n.a.	50	0.4	−0.2	−0.2	048/83	188/06	279/05	0.07	18	0.37	12	0.3	
025/06W	LDR	40	0.2	−0.1	−0.1	067/84	229/06	319/01	0.03	22.5	0.21	11	0.2	N
A6	n.a.	50	0.9	−0.1	−0.8	199/68	41/21	308/08	0.12	34	0.3	37	0.8	
020/06W	LDR	40	0.5	0.0	−0.5	208/63	35/27	304/02	0.05	27.5	0.16	34	0.5	N
A7	n.a.	50	1.3	0.2	−1.5	045/40	188/45	298/19	0.57	34	0.42	40	1.4	
024/07W	LDR	40	0.5	0.2	−0.7	042/48	201/40	300/10	0.13	30	0.23	36	0.6	N

[a] LDR — 20% of largest deviations removed; n.a. — not applicable, N — northern domain, T — transitional domain.
[b] With bedding horizontal.

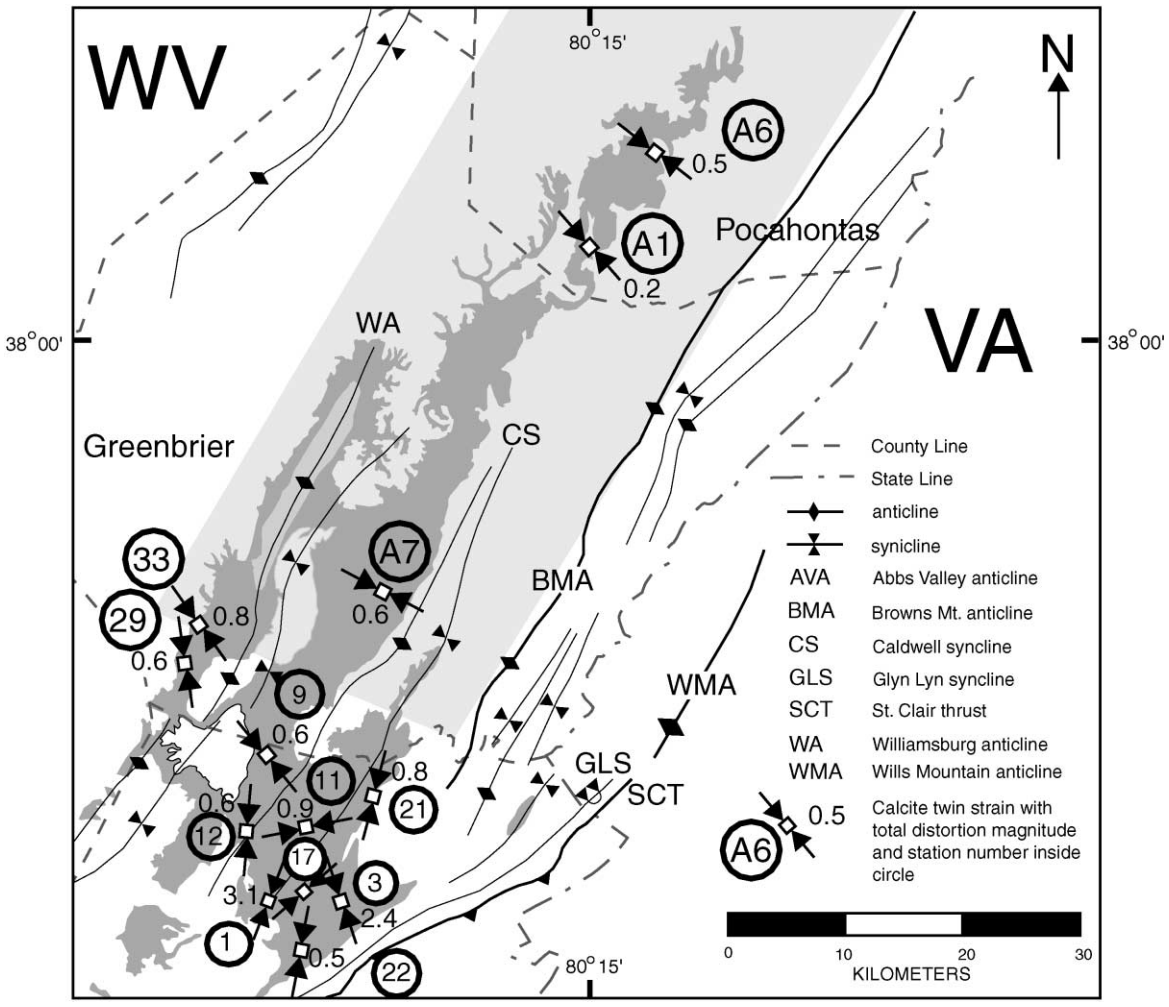

Fig. 12. Map showing calcite twin-strain magnitudes and shortening directions in the transitional and northern domains (see Table 2).

the geometry of the *Z*-axes. Assuming that pretectonic compaction was a uniaxial flattening with the short axis of the strain ellipsoid normal to bedding, bedding-parallel strain ellipses would be circular after compaction. Thus, thin sections oriented parallel to bedding were analyzed to measure layer-parallel strain (LPS) that followed the compactional event.

In the southern domain, we collected two samples that both have short ellipse axes that are locally normal to the axes of their host folds (Table 3, Fig. 7). The ellipticities (R) of the bed-parallel ellipses are 1.06 and 1.15.

The transitional domain, consisting of ten samples, again has a complex pattern of shortening directions as interpreted from the trends of the short axes of the bedding-parallel strain ellipses (Table 3, Fig. 7). Five ellipses have short axes with a N to NE trend, that is nearly strike-parallel, ranging from 11 to 45° with an average of $27 \pm 13°$ (Table 3). These samples have R values from 1.02 to 1.14 with an average of 1.07 ± 0.05. Another three ellipses have short axes with trends oblique to southern and central Appalachian shortening directions with orientations ranging from 301 to 317° and R values from 1.03 to 1.14. The two remaining ellipses have short axes with a NNW trend of 337 and 345°, and R values of 1.10 and 1.21, respectively.

Three of the five samples from the northern domain have short axes normal to map-scale central Appalachian axial traces with an average of $298 \pm 5°$, and low R values of 1.03–1.07. The two remaining samples have short axes oriented at 327 and 329° with small R values of 1.02 and 1.07, respectively.

4.3.1. Magnitude of LPS as a function of volume loss

Because twinning strains are small, R values for the strain ellipses in bedding were treated as being a result of volume loss. Assuming plane strain because of the lack of extension structures, elongations were calculated (Table 3). Shortening magnitudes range from 2 to 17% with the smallest overall strains occurring in the northern domain.

5. Discussion

5.1. Spatial and temporal distribution of shortening directions

For the southern domain, short axes of strain ellipses,

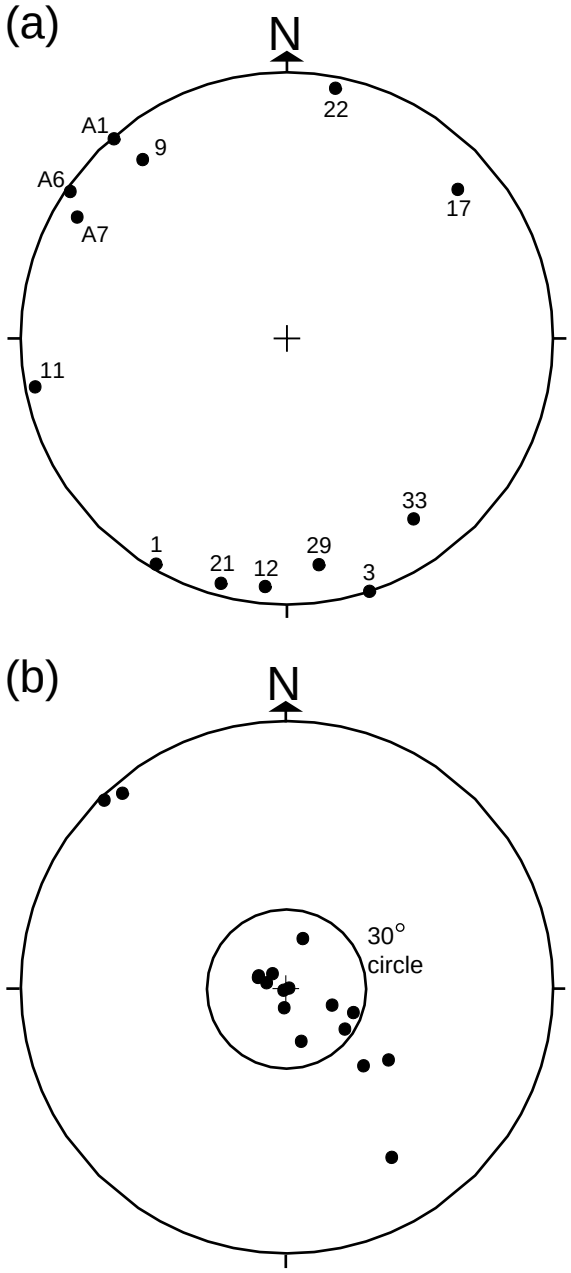

Fig. 13. (a) Equal-area lower hemisphere projection of calcite twin short (e_3) axes for NEV population with bedding rotated to the horizontal about bedding strike (number = station number). (b) Equal-area lower hemisphere projections of principal strain ellipsoid short (Z) axes determined by normalized Fry method with bedding rotated to the horizontal.

stylolitic columns and the trend of map-scale structures are all consistent with the simple interpretation that they resulted from a single southern Appalachian shortening event on the southeast flank of the Roanoke recess.

For the northern domain, interpreted shortening directions record a slightly more complex deformation history. Stylolitic cleavage records an average shortening direction of 318 ± 7° that is oblique to both southern and central Appalachian regional shortening directions (Table 2, Fig. 9). Eight of 29 orientation measurements fall within the range of southern Appalachian shortening directions, but none fall within the range of central Appalachian shortening directions despite being contained in the limbs of the central Appalachian folds. The cleavage is bed-normal and contained in fold limbs that lack noticeable lithological differences and evidence of bedding-parallel slip. Dean et al. (1988) interpreted this situation to mean that cleavage formed before folding in response to bed-parallel maximum compression rather than during folding, which would require local stress refraction to produce a maximum compression locally parallel to bedding but not normal to fold axes. We agree with this interpretation, and the result that the cleavage is older than the folds. The shortening directions from Fry plots show both southern and central trends (Table 3, Fig. 7). The twins record shortening directions subnormal to the fold axes (Table 2, Fig. 12). Thus, the northeastern flank of the Roanoke recess records an earlier NW-directed shortening in the stylolitic cleavage and grain-scale deformation that is overprinted by shortening of a central Appalachian trend that is recorded by map-scale folds, twins and grain-scale solution structures.

The transitional domain is more complex still. The stylolitic cleavage, twins and Fry plots locally record a near N–S shortening trend, which is the oldest shortening direction recorded by the cleavage in the domain. Again, all indicators record a NW–SE shortening trend that is oblique to both southern and central Appalachian regional shortening directions, although the magnitude of shortening decreases to the southwest from the northern into the transitional domain. Only twins and a few stylolites found by Dean et al. (1988, p. 309) locally record an E–W shortening trend. Dean et al. (1988) argued on the basis of geometry that these stylolites are the youngest in the area. Also, only the grain-scale solution structures locally record shortening parallel to the trend of the central Appalachian folds as measured by the Fry method. Thus, in the transitional domain, shortening directions are recorded over an arc of greater than 90°, although smaller scale indicators do not record shortening trends specifically parallel to the southern and central Appalachian shortening directions.

Deformation is heterogeneously distributed in space in the domain (Figs. 7, 9, 11 and 12), indicating that, locally, rocks only accommodated portions of the deformation. Given that deformation likely occurred at less than 200°C based on conodont color alteration indices of 2.0–3.0 from the Greenbrier Group (Epstein et al., 1977; Harris et al., 1978, 1994), this spatial heterogeneity probably reflects the fact that stylolitic columns, twins and grain-to-grain sutures are difficult structures to alter once emplaced (Groshong, 1976, 1988; Burkhard, 1993; Dunne and Caldanaro, 1997). For example, overprinting of stylolites in the study area required formation of a second set of solution surfaces rather than direct modification of the existing stylolitic columns (Fig. 10). Also, twins were seldom kinked by other twins, or bent by unseen dislocation-slip surfaces. The twins additionally show the typical intensities and sizes

Table 3
Fry analyses bedding plane ellipse data

Sample number	R	Volume loss[a] (%)	Shortening direction[b]	Domain	Trend
30	1.06	− 6	341	Southern	Southern
32	1.02	− 2	325	Southern	Southern
1	1.14	− 13	11	Transitional	Strike-parallel
4	1.03	− 3	26	Transitional	Strike-parallel
21	1.05	− 5	18	Transitional	Strike-parallel
22	1.06	− 6	35	Transitional	Strike-parallel
29	1.11	− 10	45	Transitional	Strike-parallel
9	1.21	− 17	345	Transitional	NW–NNW
12	1.10	− 9	337	Transitional	NW–NNW
13	1.14	− 12	301	Transitional	WNW–NW
17	1.03	− 3	317	Transitional	WNW–NW
33	1.07	− 6	308	Transitional	WNW–NW
23	1.02	− 2	327	Northern	Southern
28	1.07	− 6	329	Northern	Southern
a1	1.03	− 3	295	Northern	Central
a6	1.07	− 6	303	Northern	Central
a7	1.03	− 3	295	Northern	Central

[a] For 100% volume loss, $R = 1/(1 -$ volume loss).
[b] Bedding restored to the horizontal.

(Table 2) expected for low-temperature twinning, when nucleation of new twins dominates over twin widening (Ferrill, 1991).

In terms of deformation sequence in the transitional domain, all types of smaller-scale shortening indicators are folded in the limbs of central Appalachian folds (Dean et al., 1988), indicating that the folds are younger. Whitaker and Bartholomew (1999), however, found that smaller-scale structures recording the NW–SE shortening trend are preserved in the overturned limb of the Glen Lyn syncline, which is a southern Appalachian structure. As a result, the inner arc of the Roanoke recess records NW–SE shortening by smaller-scale structures preceding any larger-scale structures of either southern or central Appalachian origin. Some smaller-scale deformation preceding larger-scale deformation is typical of low-temperature limestone deformation in foreland thrust belts (Groshong, 1976; Marshak and Engelder, 1985; Craddock and van der Pluijm, 1989; Holl and Anastasio, 1995).

This analysis reduces to a few key temporal relationships that form the basis for the interpretation in the next section:

1. N-directed stylolitic teeth precede NW-directed stylolitic teeth (this study).
2. NW-directed stylolitic cleavage is older than both folds with southern and central Appalachian trends (Dean et al., 1988; Whitaker and Bartholomew, 1999; this study).
3. WNW-directed small-scale structures are interpreted to be the same age as host central Appalachian folds because their axes are normal to this shortening direction (Dean et al., 1988; this study).
4. W-directed stylolitic teeth are the youngest structures (Dean et al., 1988).

5.2. Evolution of the Roanoke recess

Combining the new data about the distribution and timing of shortening with the existing observations that larger-scale structures deform smaller ones (Dean et al., 1988; Whitaker and Bartholomew, 1999) leads to a revised interpretation about the deformation history at this recess. The essence of this reinterpretation is that the deformation was a continuum in time. Previous investigators have focused on establishing the relative order of the southern and central Appalachian deformation in the recess with the idea that the history would be two-step. We believe that establishing the deformation sequence does not require a step-like history with interludes of no deformation. Instead, a continuous deformation with temporally fluctuating intensity is quite likely in a large-scale tectonic process, such as the terminal Alleghanian collision that involved the Roanoke recess.

Evidence for discounting a two-step deformation history includes:

1. NW-trending cleavage with one orientation is overprinted by southern and central Appalachian map-scale structures that have different trends from each other and the cleavage.
2. Continuity of map-scale structures around the recess, such as the Staunton–Pulaski fault system or the anticline at the NE termination of the St. Clair thrust into the Wills Mountain anticline (Butts, 1933, 1973; Calver, 1963; Rodgers, 1970; Bartholomew, 1981, 1987).
3. Map-scale structures of these two trends do not produce interference patterns, which would be expected for sequential overlapping map-scale structures. A possible exception was identified by Bick (1986), but has been

descredited by Bartholomew (pers. commun.; Whitaker and Bartholomew, 1999).

The only surviving direct evidence for a two-step deformation would be that central Appalachian structures deform younger rocks and that a few structures such as the Rich Patch anticline have an oblique structural trend at the intersection of the two trends (Rodgers, 1970). However, the age difference of the deformed rocks could be an artifact of erosional differences. The oblique structures lack interference patterns and may just represent a locally segmented rather than smoothly curving structural geometry around the recess. Consequently, no compelling evidence exists for a two-step deformation history.

Discarding a two-step interpretation for the deformation history of the recess, a new interpretation needs to incorporate the following observations:

1. The deformation occurred at a pre-existing promontory (Thomas, 1977; Hatcher et al., 1989).
2. To the south of the recess, all structures record a coaxial deformation.
3. The structural sequence to the north of the recess is outcrop-scale cleavage and microscale solution surfaces with NW-directed shortening followed by map-scale and microscale structures with WNW-directed shortening typical of central Appalachian deformation.
4. Cleavage with NW-directed shortening is found in the center (transitional domain) and to the north of the recess. In the center, it is folded by map-scale southern Appalachian structures (Whitaker and Bartholomew, 1999).
5. Structures in the center of the recess record a series of shortening directions from oldest N-directed (stylolitic teeth) to NW-directed (stylolitic teeth) to NNW-directed and WNW-directed (map-scale structures) to W-directed (stylolitic teeth).
6. In the center, the variety and ages of shortening directions do not have a spatial arrangement consistent with simple bending about the recess (Fig. 2 vs. Figs. 7, 9, 11 and 12).

We interpret these observations to represent a progressive deformation around a recess where the center of the deformation intensity migrates northeastward around the recess. We will present this interpretation as stages, but these stages are just a convenient means for illustrating the highlights of the deformation history as opposed to representing discrete time steps:

Stage 1: Deformation initiated to the south of the recess as NNW-directed shortening and spread into the recess as N-directed shortening.

Stage 2: Deformation continued coaxially in the south, while both the center and northern flank of the recess developed cleavage with NW-directed shortening. A key question is why this new deformation was NW-directed rather than NNW-directed as it was to the south. The data do not contain the basis for a definitive answer. We offer the possibility that the existence of the promontory caused an anticlockwise refraction of displacement directions.

Stage 3: Deformation continued with map-scale structures folding the cleavage in both the center and the northern flank of the recess. The map-scale structures changed from a southern Appalachian trend to a central Appalachian trend northeastward. They lack overprinting relationships and some are large laterally continuous through the two trends. We interpret the continuity and the lack of overprinting as evidence for northeastward propagation of the map-scale structures as the deformation center migrated in the same direction. Deformation could have continued to the south during this time, but the data do not contain evidence to support or refute this contention.

Stage 4: The deformation center migrated around the recess so that deformation was then concentrated to the north of the recess, producing the late-stage, localized W-directed deformation recorded by cleavage in the recess center (Dean et al., 1988) and continued the WNW-directed deformation to the north at all scales. In the area south of the recess, evidence is lacking for a structural overprint at this stage, perhaps due to insufficient deformation intensity, or because for these low-temperature conditions, the available energy is insufficient to the task of deforming rocks that already contain thrusts, folds, cleavage and smaller-scale structures.

Models for salient development (Fig. 1) (e.g. Marshak, 1988; Hindle and Burkhard, 1999), typically have 'centers of deformation' such that the axis of maximum displacement for the finite deformation is coincident with the axes for incremental maximum displacement. Put differently, the displacement field evolves symmetrically with a fixed axis of maximum displacement that reflects an assumed continuity of boundary conditions and initial geometric characteristics (Macedo and Marshak, 1999; Hindle and Burkhard, 1999). In contrast, the Roanoke recess preserves a strain pattern that is asymmetric spatially and temporally. Our interpretation hypothesizes that this asymmetry of the strain pattern is a result of asymmetry in the displacement pattern. We believe that the displacement pattern was asymmetric around the recess throughout Alleghanian deformation and that the axis of maximum displacement migrated NE through time. As a result, an attempt to classify our interpretation in terms of general models (orocline or primary arc) (Marshak, 1988; Hindle and Burkhard, 1999) will fail because the deformation pattern in the recess does not match the kinematic assumptions for these models.

The Roanoke recess may be viewed as a pre-existing buttress that was not a depocenter around which the deformation center changed position through time. Several possibilities exist for the cause of this proposed moving

deformation pattern. One is that the center may have been the migrating point of maximum impact between Laurentia and Gondwanaland (Geiser and Engelder, 1983; Sacks and Secor, 1990). Another is that segmentation of Gondwanaland by faults changed indenter geometry. Yet another is the possibility of a changing spatial distribution of the mechanical strength of the basal detachment beneath the orogen through time. No doubt other possibilities exist, and while resolving this choice is beyond the scope of the present contribution, the presence of many possibilities supports the new interpretation.

Our interpretation argues for the Roanoke recess not being an intersection recess like the Kingston recess (Marshak and Tabor, 1989). Instead, deformation was continuous during a single orogenic event, and the displacement maximum migrated rather than being bimodal or stationary as with the Kingston recess.

Comparing the proposed deformation history of the Roanoke recess to the Pennsylvania salient shows that these two tectonic features did not experience 'mirror' deformations. The Pennsylvania salient records an orderly pattern of shortening directions rotating out from the center. In the center of the salient in the Juniata culmination, deformation is coaxial through time with shortening oriented between 322 and 340° (Nickelsen and Engelder, 1989; Spiker and Gray, 1997). A counterclockwise Alleghanian stress field rotation is indicated to the south (Nickelsen and Hough, 1967; Nickelsen, 1988; Evans, 1994) and a clockwise stress field rotation indicated to the north of this culmination (Engelder and Geiser, 1979; Nickelsen, 1979; Gray and Mitra, 1993; Younes and Engelder, 1999). Deformation appears to be active throughout the salient at all stages. In contrast, deformation progressed northeastward in the Roanoke recess during an overall anticlockwise rotation of the shortening direction from N to W. Thus, while the recess and salient may have formed in response to the same bulk plate tectonic behavior, they pursued unique deformation histories to achieve their present forms.

5.3. Existence of a blind detachment

The St. Clair fault, which has up to 20 km displacement, terminates in a regional anticline at the junction of the southern and central Appalachians. Couzens and Dunne (1994) suggested that this termination is the result of displacement transfer to a blind thrust instead of simply a displacement decrease to zero for an emergent thrust (Dahlstrom, 1969). Their hypothesis would require up to 20 km of shortening to be accommodated by Plateau rocks above a proposed thrust flat that is to the foreland of the surface trace of the St. Clair fault (Fig. 6).

Measurements of stylolite amplitudes for a minimum shortening estimate from the cleavage, and bedding-plane finite strain ellipses for a shortening estimate within cleavage microlithons are used to quantify the shortening magnitude across the interior of the recess (Tables 1, 3 and 4, Fig. 6). These shortening magnitudes vary along the section, but show no systematic pattern that would necessitate data partitioning. Therefore, average values calculated for the strains across the cleavage zones and microlithons are added to the map-scale shortening estimate from the cross-section to provide a more accurate estimate of total shortening (Dunne, 1996). To average the shortening magnitudes, each shortening vector must be resolved into its component along the 150–330° section (Table 4). This calculation is possible for these finite strains because their magnitudes are measured as a 100% volume loss, yielding vectors with unique shortening directions. So, vector magnitudes along section are determined by multiplying the cosine of the angular difference between trend of the section and measured elongation vector. Cleavage shortening magnitudes along this cross-section slightly decrease toward the foreland, averaging 4.9% across the entire section. Shortening calculated from ratios of the strain ellipses are 4.9%, assuming 100% volume loss. Shortening calculated with a line-length comparison for the map-scale folds equals 4.7%.

Using the initial bed length previously determined for the Greenbrier limestone of 28.3 km, the combined shortening percentage of 14.5% represents 4.1 km of shortening. Therefore, total shortening as resolved parallel to 330° almost exceeds 15%, which is quite comparable with shortening magnitudes recorded to the north in the central Appalachian Plateau (Engelder and Engelder, 1977; Smart et al., 1997). This magnitude of shortening does necessitate a blind floor thrust beneath the study area that formed before or during the onset of the stylolitic cleavage with NW-oriented teeth (Engelder and Engelder, 1977). This 4.1 km of shortening is significantly less than the 20 km of displacement for the St. Clair thrust, so if displacement transfer occurred along a blind thrust flat beneath the St. Clair thrust, significant shortening would have to be present further into the foreland. For example, accommodation of 20 km of displacement would require deformation across 130 km of the Plateau at the same shortening magnitude (14.5%) as measured in the study area, or smaller magnitudes distributed over a longer distance. It is worth noting that Craddock and van der Pluijm (1989) have measured 1–2% calcite-twin strains in the Michigan basin that they attribute to Appalachian deformation. Therefore, while it is likely that an Alleghanian blind thrust is under the Greenbrier Group rocks of the Plateau, it is not clear that this fault accommodated as much of the displacement of the St. Clair thrust sheet as Couzens and Dunne (1994) envisioned.

Still, we believe that the existence of this blind flat supports the interpretation that the St. Clair thrust sheet and the thrust horse under the Wills Mountain anticline are one structure (Wilson and Shumaker, 1992; Couzens and Dunne, 1994). Our reasons are that the flat underlies structures related to emplacement of both the thrust sheet and horse (Figs. 7, 9, 11 and 12), and connects by branch lines to both structures (Fig. 3).

Table 4
Corrected shortening values for data from stylolitic cleavage and normalized Fry method

Cleavage data

Station number	Cleavage rotated[a]	Teeth orientation (°)	Measured shortening	Corrected shortening along 330
54	049/70	319	4.8	4.7
55	046/75	316	6.7	6.5
56	049/78	319	7.4	7.3
57	060/86	330	3.8	3.8
61	044/84	360	5.1	4.4
2	218/83	308	7.4	6.9
3	041/86	311	5.7	5.4
5	214/83	304	6.5	5.8
6	047/89	317	1.6	1.6
8	051/84	320	7.0	6.9
9	049/87	319	5.7	5.6
32	228/89	318	4.8	4.7
43	228/84	318	7.0	6.8
63	225/80	315	3.2	3.1
4	215/86	340	5.7	5.6
7	121/82	350	5.3	5.0
29	217/89	355	7.4	6.7
30	217/89	355	8.3	7.5
31	038/90	350	3.8	3.6
33	040/90	350	5.7	5.4
34	045/90	350	3.8	3.6
35	045/90	350	4.6	4.3
46	220/84	360	4.1	3.6
47	054/90	360	5.7	4.9
62	226/81	355	4.8	4.4
70	045/82	315	3.1	3.0
71	045/90	315	5.7	5.5
72	047/87	317	2.4	2.3
73	230/86	320	2.4	2.4
Average:			5.2 ± 1.7%	4.9 ± 1.6%

Fry method

Sample number	Ellipticity ratio (R)	Trend[b] (°)	Measured shortening	Corrected shortening along 330
17	1.03	317	3.0	2.9
22	1.06	35	6.0	2.5
1	1.14	11	13.0	9.8
4	1.03	26	3.0	1.7
12	1.1	337	9.0	8.9
29	1.11	45	10.0	2.6
33	1.07	308	6.0	5.6
Average:			7.1 ± 4%	4.9 ± 3%

[a] Bedding rotated to the horizontal.
[b] Trend of shortening axis with bedding rotated to the horizontal.

6. Conclusions

1. The inner arc of the Roanoke recess in the Appalachian Plateau records Alleghanian deformation from micro-scale to map-scale that displays shortening directions ranging over greater than 90° and a total percentage magnitude near 15%.
2. The array of shortening directions and relative age of the structures are interpreted to be the result of the progressive northeastward migration of the center of deformation around a pre-existing promontory. The deformation pattern is asymmetric with a progressive counterclockwise rotation of the shortening direction through time that is not the mirror of the deformation pattern to the north in the Pennsylvania salient where deformation is symmetric and shortening directions rotate progressively outward through time.
3. The shortening magnitude of about 15% (locally 4.1 km of shortening) necessitates an underlying blind decollement. Yet, this blind flat has not locally accommodated the 20 km displacement of the adjacent St. Clair thrust sheet. For such an accommodation to occur, additional deformation would need to be present further into the

foreland. The existence of the blind fault supports an interpretation that the St. Clair thrust sheet and the Wills Mountain duplex are a continuous structure.

Acknowledgements

Financial support to this project was provided to Alan Spraggins by a grant from the Southeastern section of the Geological Society of America and a Grant-in-Aid of Research from Sigma Xi. Earlier versions were improved by comments from Bob Hatcher, Brent Couzens-Schultz, and Kevin Smart, and journal reviewers David Wiltschko and Jim Evans.

References

Alvarez, W., Engelder, T., Geiser, P.A., 1978. Classification of solution cleavage in pelagic limestones. Geology 6, 263–266.

Bartholomew, M.J., 1981. Geology of the Roanoke and Stewartsville quadrangles, Virginia. Virginia Division of Mining Resources Publication, 34.

Bartholomew, M.J., 1987. Structural evolution of the Pulaski thrust system, southwestern Virginia. Virginia Division of Mineral Resources, 34.

Bick, K.F., 1986. Structure of the Sugarloaf Mountain area: intersecting trends on the northeast flank of the Roanoke reentrant, Virginia. In: Mcdowell, R.C., Glover III, L., Rodgers, J., Bambach, R.K., Gray, D.R. (Eds.). The Lowry Volume: Studies in Appalachian Geology. Virginia Polytechnic Institute and State University, Department of Geological Sciences, Memoir 3, pp. 27–36.

Burkhard, M., 1993. Calcite twins, their geometry, appearance and significance as stress-strain markers and indicators of tectonic regime: a review. Journal of Structural Geology 15, 351–358.

Butts, C., 1933. Geological map of the Appalachian Valley in Virginia. Virginia Geological Survey, scale 1:250,000.

Butts, C., 1973. Geology of the Appalachian Valley in Virginia, Part 1: geologic text and illustrations. Virginia Division of Mineral Resources Bulletin 52.

Calver, J.L., 1963. Geologic Map of Virginia. Virginia Division of Mineral Resources, scale 1:500,000.

Cardwell, D.H., Erwin, R.B., Woodward, H.P., 1968. 1968 Geologic map of West Virginia. West Virginia Geological and Economic Survey, 1:250,000.

Carey, S.W., 1955. The orocline concept in geotectonics. Paper and Proceedings of the Royal Society of Tasmania 89, 255–289.

Cloos, E., 1947. Oolite deformation in the South Mountain fold, Maryland. Geological Society of America Bulletin 58, 843–917.

Couzens, B.A., Dunne, W.M., 1994. Displacement transfer at thrust terminations: the Saltville thrust and Sinking Creek anticline, Virginia, USA. Journal of Structural Geology 16, 781–793.

Craddock, J.P., van der Pluijm, B.A., 1989. Late Paleozoic deformation of the cratonic carbonate cover of eastern North America. Geology 17, 416–419.

Dahlstrom, C.D.A., 1969. Balanced cross-sections. Canadian Journal of Earth Sciences 6, 743–760.

Dean, S.L., Kulander, B.R., Skinner, J.M., 1988. Structural chronology of the Alleghanian orogeny in southeastern West Virginia. Geological Society of America Bulletin 100, 299–310.

Dunham, R.J., 1962. Classification of carbonate rocks according to depositional texture. Memoir — American Association of Petroleum Geologists, 108–121.

Dunne, W.M., 1996. The role of macroscale thrusts in the deformation of the Alleghanian roof sequence in the central Appalachians: a re-evaluation. American Journal of Science 296, 549–575.

Dunne, W.M., Caldanaro Jr, A.J., 1997. Evolution of solution structures in a deformed quartz arenite: geometric changes related to permeability changes. Journal of Structural Geology 19, 663–672.

Engelder, T., Engelder, R., 1977. Fossil distortion and decollement tectonics of the Appalachian Plateau. Geology 5, 457–460.

Engelder, T., Geiser, P.A., 1979. The relationship between pencil cleavage and lateral shortening within the Devonian section of the Appalachian Plateau, New York. Geology 7, 460–464.

Epstein, A.G., Epstein, J.B., Harris, L.D., 1977. Conodont color alteration — an index to organic metamorphism. United States Geologic Survey Professional Paper 995, 27p.

Erslev, E.A., 1988. Normalized center-to-center strain analysis of packed aggregates. Journal of Structural Geology 10, 201–209.

Evans, M.A., 1994. Joints and decollement zones in Middle Devonian shales: Evidence for multiple deformation events in the Central Appalachian Plateau. Geological Society of America Bulletin 106, 447–460.

Evans, M.A., Groshong Jr, R.H., 1994. A computer program for the calcite strain-gauge technique. Journal of Structural Geology 16, 277–281.

Ferrill, D.A., 1991. Calcite twin widths and intensities as metamorphic indicators in natural low-temperature deformation of limestone. Journal of Structural Geology 13, 667–675.

Ferrill, D.A., Groshong Jr, R.H., 1993a. Kinematic model for the curvature of the northern Subalpine Chain, France. Journal of Structural Geology 15, 523–541.

Ferrill, D.A., Groshong Jr, R.H., 1993b. Deformation conditions in the northern Subalpine Chain, France, estimated from deformation modes in coarse-grained limestone. Journal of Structural Geology 15, 995–1006.

Fletcher, R.C., Pollard, D.D., 1981. Anticrack model for pressure solution surfaces. Geology 9, 419–424.

Fry, N., 1979. Random point distributions and strain measurement in rock. Tectonophysics 60, 89–105.

Geiser, P.A., Sansone, S., 1981. Joints, microfractures, and the formation of solution cleavage in limestone. Geology 9, 280–285.

Geiser, P.A., Engelder, T., 1983. The distribution of layer parallel shortening fabrics in the Appalachian foreland of New York and Pennsylvania: evidence for two noncoaxial phases of Allaghanian orogeny. In: Hatcher Jr, R.D., Williams, H., Zeitz, I. (Eds.). Contributions to the Tectonics and Geophysics of Mountain Chains. Geological Society of America Memoir 158, pp. 161–175.

Gray, M.B., Mitra, G., 1993. Migration of deformation fronts during progressive deformation: Evidence from detailed structural studies in the Pennsylvania Anthracite region, USA. Journal of Structural Geology 15, 435–449.

Gray, M.B., Stamatakos, J., 1997. New model for evolution of fold and thrust belt curvature based on integrated structural and paleomagnetic results from the Pennsylvania salient. Geology 25, 1067–1070.

Groshong Jr, R.H., 1972. Strain calculated from twinning in calcite. Geological Society of America Bulletin 83, 2025–2038.

Groshong Jr, R.H., 1974. Experimental test of least-squares strain gage calculation using twinned calcite. Geological Society of America Bulletin 86, 1855–1864.

Groshong, R.H., 1976. Strain and pressure solution in the Martinsburg Slate, Delaware Water Gap, New Jersey. American Journal of Science 276, 1131–1146.

Groshong Jr, R.H., 1988. Low-temperature deformation mechanisms and their interpretation. Geological Society of America Bulletin 100, 1329–1360.

Groshong Jr, R.H., Teufel, L.W., Gasteiger, C., 1984a. Precision and accuracy of the calcite strain-gage technique. Geological Society of America Bulletin 95, 357–363.

Groshong Jr, R.H., Pfiffner, O.A., Pringle, L.R., 1984b. Strain partitioning in the Helvetic thrust belt of eastern Switzerland from the leading edge to the internal zone. Journal of Structural Geology 6, 5–18.

Gwinn, V.E., 1964. Thin-skinned tectonics in the Plateau and northwestern

Valley and Ridge provinces of the central Appalachians. Geological Sociey of America Bulletin 75, 863–900.

Harris, A.G., Harris, L.D., Epstein, J.B., 1978. Oil and gas data from Paleozoic rocks in the Appalachian basin: maps for assessing hydrocarbon potential and thermal maturity (conodont color alteration isograds and overburden isopachs). US Geological Survey Miscellaneous Investigation Series I-917-E, scale 1:2,500,000.

Harris, A.G., Stamm, N.R., Weary, D.G., Repetski, J.E., Stamm, R.G., Parker, R.A., 1994. Conodont color alteration index (CAI) map and conodont-based age determinations for the Winchester $30' \times 60'$ quadrangle and adjacent area. Virginia, West Virginia, and Maryland. US Geological Survey Miscellaneous Field Studies Map MF-2239, scale 1:100,000.

Hatcher Jr, R.D., Thomas, W.A., Geiser, P.A., Snoke, A.W., Mosher, S., Wiltschko, D.W., 1989. Alleghanian orogen. In: Hatcher Jr, R.D., Thomas, W.A., Viele, G.W. (Eds.). The Appalachian–Ouachita Orogen in the United States. , pp. 233–318 Geological Society of America, The Geology of North America F-2.

Hindle, D., Burkhard, M., 1999. Strain, displacement and rotation associated with the formation of curvature in fold belts; the example of the Jura Arc. In: Evans, J.P., Treagus, S.H. (Eds.), Questions in Structural Geology; 20th Anniversary Special Issue. Journal of Structural Geology 21, 1089–1101.

Holl, J.E., Anastasio, D.J., 1995. Cleavage development within a foreland fold and thrust belt, southern Pyrenees, Spain. Journal of Structural Geology 17, 357–369.

Kulander, B.R., Dean, S.L., 1986. Structure and tectonics of central and southern Appalachian Valley and Ridge and Plateau Provinces, West Virginia and Virginia. American Association of Petroleum Geologists Bulletin 70, 1674–1684.

Macedo, J., Marshak, S., 1999. Controls on the geometry of fold-thrust belt salients. Geological Society of America Bulletin 111, 1808–1822.

Marshak, S., 1988. Kinematics of orocline and arc formation in thin-skinned orogens. Tectonics 7, 73–86.

Marshak, S., Engelder, T., 1985. Development of cleavage in limestones of a fold-thrust belt in eastern New York. In: Hancock, P.L., Powell, C. McA. (Eds.), Multiple Deformation in Ductile and Brittle Rocks. Journal of Structural Geology 7, 345–359.

Marshak, S., Tabor, J.R., 1989. Structure of the Kingston Orocline in the Appalachian fold-thrust belt, New York. Geological Society of America Bulletin 101, 683–701.

Marshak, S., Flöttmann, T., 1996. Structure and origin of the Fleurieu and Nackara arcs in the Adelaide fold-thrust belt, South Australia; salient and recess development in the Delamerian Orogen. Journal of Structural Geology 18, 891–908.

Means, W.D., 1976. Stress and Strain: Basic Concepts in Continuum Mechanics for Geologists. Springer-Verlag, New York.

Meyer, T.J., Dunne, W.M., 1990. Deformation of Helderberg limestones above the blind thrust system of the Central Appalachians. Journal of Geology 98, 108–117.

Muehlberger, W.R., 1992. The tectonic map of North America, Southeast Sheet American Association of Petroleum Geologists, scale 1:5,000,000.

Nickelsen, R.P., 1979. Sequence of structural stages of the Alleghany Orogeny, at the Bear Valley strip mine, Shamokin, Pennsylvania. American Journal of Science 279, 225–271.

Nickelsen, R.P., 1988. Structural evolution of folded thrusts and duplexes on a first-order anticlinorium in the Valley and Ridge Province of Pennsylvania. In: Mitra, G., Wojtal, S.F. (Eds.), Geometries and Mechanism of Thrusting, with Special reference to the Appalachians. Special Paper—Geological Society of America 222, 89–106.

Nickelsen, R.P., Hough, V.N.D., 1967. Jointing in the Appalachian Plateau of Pennsylvania. Geological Society of America Bulletin 78, 609–629.

Nickelsen, R.P., Engelder, T., 1989. Day 4; Fold-thrust geometries of the Juniata Culmination, Central Appalachians of Pennsylvania. In: Hanshaw, P.M. (Ed.). Metamorphism and Tectonics of Eastern and Central North America; Volume 2, Structures of the Appalachian Foreland Fold-thrust Belt. American Geophysical Union, pp. 35–43.

Ogden, A.E., 1976. The Hydrogeology of the central Monroe County Karst, West Virginia. Ph.D. thesis, West Virginia University, Morgantown.

Onasch, C.M., Dunne, W.M., 1993. Variation in quartz arenite deformation mechanisms betweena roof sequence and duplexes. Journal of Structural Geology 15, 465–475.

Owens, W.H., 1984. The calculation of a best-fit ellipsoid from elliptical sections on arbitrarily oriented planes. Journal of Structural Geology 6, 571–578.

Perry, W.J., 1978. Sequential deformation in the central Apalachians. American Journal of Science 278, 518–542.

Powell, C.McA., 1979. A morphological classification of rock cleavage. Tectonophysics 58, 21–34.

Price, P.H., 1929. Pocahontas County. West Virginia Geological Survey, 501p., 2 maps.

Price, P.H., Heck, E.T., 1939. Greenbrier County. West Virginia Geological and Economic Survey, 846p., 2 maps.

Protzman, G.M., Mitra, G., 1990. Strain fabric associated with the Meade thrust sheet: implications for cross-section balancing. Journal of Structural Geology 12, 403–417.

Reger, D.B., Price, P.H., 1926. Mercer, Monroe and Summers Counties. West Virginia Geological Survey, 963p., 3 maps.

Ries, A.C., Shackleton, R.M., 1976. Patterns of strain variation in arcuate fold belts. Philosophical Transactions of the Royal Society of London, Series A: Mathematical and Physical Sciences 283, 281–288.

Rodgers, J., 1970. The Tectonics of the Appalachians. John Wiley and Sons, New York.

Sacks, P.E., Secor, D.T., 1990. Kinematics of Late Paleozoic continental collision between Laurentia and Gondwana. Science 250, 1702–1705.

Schmid, S.M., Panozzo, R., Bauer, S., 1987. Simple shear experiments on cacite rocks; rheology and microfabric. In: Cobbold, P.R., Gapais, D., Treagus, S.H. (Eds.), Shear CRITERIA in Rocks. Journal of Structural Geology 9, 747–748.

Skinner, J.M., 1979. A paleostress analysis of the Greenbrier Group (Mississippian), Monroe County, West Virginia. M.S. thesis, University of Toledo.

Smart, K.J., Dunne, W.M., Krieg, R.D., 1997. Roof sequence response to emplacement of the Wills Mountain duplex: the roles of forethrusting and scales of deformation. Journal of Structural Geology 19, 1443–1459.

Spiker, E.C., Gray, M.B., 1997. A study of progressive deformation at the Allegheny Front, Lycoming County, PA. Abstracts with Programs — Geological Society of America 29, 82.

Stockdale, P.B., 1922. Stylolites: their nature and origin. Indiana University Studies, 55.

Thomas, W.A., 1977. Evolution of Appalachian–Ouachita salients and recesses from reentrants and promontories in the continental margin. American Journal of Science 277, 1233–1278.

Whitaker, A.E., Bartholomew, M.J., 1999. Layer parallel shortening: a mechansim for determining deformation timing at the junction of the central and southern Appalachians. American Journal of Science 299, 238–254.

Wilson, T.H., Shumaker, R.C., 1992. Broad Top thrust sheet: an extensive blind thrust in the central Appalachians. American Association of Petroleum Geologists Bulletin 76, 1310–1324.

Woodward, N.B., 1985. Valley and Ridge thrust belt: balanced structural sections, Pennsylvania to Alabama. University of Tennessee Studies in Geology, 12.

Younes, A.I., Engelder, T., 1999. Fringe cracks; key structures for the interpretation of the progressive Alleghanian deformation of the Appalachian Plateau. Geological Society of America Bulletin 111, 219–239.